RESEARCH ARTICLE | JULY 09 2025

The energy denominator effect in lambda-doubling

Robert J. Gordon ; Robert W. Field

J. Chem. Phys. 163, 024313 (2025)
https://doi.org/10.1063/5.0277788

The Journal of Chemical Physics ARTICLE pubs.aip.org/aip/jcp

The energy denominator effect in lambda-doubling

Cite as: J. Chem. Phys. 163, 024313 (2025); doi: 10.1063/5.0277788
Submitted: 25 April 2025 • Accepted: 11 June 2025 •
Published Online: 9 July 2025

Robert J. Gordon[1,a)] and Robert W. Field[2]

AFFILIATIONS

[1] Department of Chemistry, University of Illinois at Chicago, Chicago, Illinois 60680, USA
[2] Department of Chemistry, Massachusetts Institute of Technology, Cambridge, Massachusetts 02139, USA

[a)] **Author to whom correspondence should be addressed:** rjgordon@uic.edu

ABSTRACT

Lambda-doubling is the lifting of the degeneracy of a pair of rotational levels of opposite e/f-symmetry, which is caused by their interaction with rotational levels of an energetically remote electronic state. Historically, this phenomenon has been associated with the symmetry dependence of the matrix elements that appear in the *numerator* of a second-order perturbation expression. We show that this effect may be present even when there is no rotational interaction or when the off-diagonal matrix element of the rotational Hamiltonian is independent of e/f-symmetry.

I. INTRODUCTION

Lambda-doubling is a feature in the rotational spectra of molecules that is indicative of electronic perturbations by energetically remote states.[1–4] Throughout its long history, Λ-doubling has been interpreted as a consequence of the e/f-symmetry of the off-diagonal matrix elements of the rotation and/or the spin–orbit terms in the Hamiltonian. In each of the contributing interactions e- and f-symmetries are an alternate way of labeling the parity quantum number.[5] In this paper, we show that Λ-doubling is a more general phenomenon that may exist even when these matrix elements are independent of e/f-symmetry. Lambda-doubling is, rather, a consequence of the symmetry properties of the *perturbation paths*, which include both numerator and denominator effects. (By "path," we mean the interaction of two states that have the same e/f-symmetry and the same total angular momentum quantum number.)

A diatomic molecule is characterized by its parity, its total angular momentum, **J**, with a projection of $\Omega\hbar$ along its internuclear axis, its total electron spin, **S**, and its projection, $\Sigma\hbar$, along that axis, and the projection, $\Lambda\hbar$, of the total orbital angular momentum. (The orbital angular momentum itself, **L**, is not well-defined for a diatomic molecule.[4]) Non-Σ electronic states are orbitally doubly degenerate, and the rotational levels may be labeled e or f according to the relation between their parity and the integer or half-integer value of J.

The symmetrized wave functions of a diatomic molecule that has an even number of electrons [see Eq. (3.2.95) of Ref. 1] are

$$|^{2S+1}\Lambda_\Omega, J\rangle_{e,f} = \frac{1}{\sqrt{2}}\left[|^{2S+1}\Lambda_\Omega\rangle|J,\Omega\rangle \pm (-1)^{-S+s}\,|^{2S+1}(-\Lambda)_{-\Omega}\rangle|J,-\Omega\rangle\right], \quad (1)$$

where $s = 1$ for Σ^- states and 0 for all other states. The ± signs correspond to e- and f-symmetries, respectively.[5] The corresponding expression for an odd number of electrons is

$$|^{2S+1}\Lambda_\Omega, J\rangle_{e,f} = \frac{1}{\sqrt{2}}\left[|^{2S+1}\Lambda_\Omega\rangle|J,\Omega\rangle \pm (-1)^{-S+s+\frac{1}{2}}\,|^{2S+1}(-\Lambda)_{-\Omega}\rangle|J,-\Omega\rangle\right]. \quad (2)$$

[The extra 1/2 term in Eq. (2) comes from the relation between e/f-symmetry and parity, as explained in Ref. 5 and p. 140 of Ref. 1.]

In the absence of a perturbation, the energies of the states described by Eqs. (1) and (2) are independent of e/f symmetry and are therefore degenerate. (An important exception is for $^2\Sigma$ states, which is discussed in Sec. V.) This degeneracy may be lifted by a perturbation by an energetically remote state of the same e- or f-symmetry. According to second-order perturbation theory, the

energy shift of the perturbed state, $|i\rangle$, by a perturbing state, $|j\rangle$, is given by

$$\delta E \equiv h\delta\nu = |\langle i|\hat{V}|j\rangle|^2/\Delta E_{ij}, \tag{3}$$

where $\hat{V}$ is the sum of the spin–orbit Hamiltonian, $\hat{\mathscr{H}}^{SO}$, and the rotational Hamiltonian, $\hat{\mathscr{H}}^{Rot}$, and $\Delta E_{ij} = E_i - E_j$ is the energy difference between the perturbed and perturbing states.

The spin–orbit Hamiltonian for n electrons is given by

$$\hat{\mathscr{H}}^{SO} = \frac{1}{2}\sum_{i=1}^{n} \hat{a}_i(\hat{\ell}_i^+\hat{s}_i^- + \hat{\ell}_i^-\hat{s}_i^+) + \sum_{i=1}^{n} \hat{a}_i\hat{\ell}_{iz}\hat{s}_{iz}, \tag{4}$$

where $\hat{a}_i$ is an r-dependent, one-electron operator that acts on the orbital angular momentum of each electron, $\hat{\ell}_i^{\pm}$ are the raising and lowering operators for the orbital angular momentum of electron i, and $\hat{s}_i^{\pm}$ are the raising and lowering operators for the spin angular momentum of electron i.

The rotational Hamiltonian is given by

$$\begin{aligned}\hat{\mathscr{H}}^{Rot} = B_{\Lambda,v_\Lambda}\{&(\hat{\mathbf{J}}^2 - \hat{J}_z^2) + (\hat{\mathbf{L}}^2 - \hat{L}_z^2) + (\hat{\mathbf{S}}^2 - \hat{S}_z^2) + (\hat{L}^+\hat{S}^- + \hat{L}^-\hat{S}^+)\\ &- (\hat{J}^+\hat{L}^- + \hat{J}^-\hat{L}^+) - (\hat{J}^+\hat{S}^- + \hat{J}^-\hat{S}^+)\}.\end{aligned} \tag{5}$$

This operator is derived from the property that the rotational angular momentum, $\mathbf{R} = J - L - S$, is perpendicular to the bond axis.[4] It is conventional to omit the $\hat{\mathbf{L}}^2 - \hat{L}_z^2$ terms, which are uncoupled from $\hat{\mathbf{J}}$ and from each other, and instead to add their expectation values to the electronic term energy. The diagonal terms in Eqs. (4) and (5) define the zeroth-order Hamiltonian in the case (a) basis set, and the off-diagonal terms in these equations lead to perturbations by remote electronic states that are responsible for Λ doubling.

It is also useful to define an operator, $\hat{\mathscr{H}}^{SU}$, which contains only the diagonal terms and the spin-uncoupling, off-diagonal terms of the rotational Hamiltonian,

$$\hat{\mathscr{H}}^{SU} = B_{\Lambda,v_\Lambda}\{(\hat{\mathbf{J}}^2 - \hat{J}_z^2) + (\hat{\mathbf{S}}^2 - \hat{S}_z^2) - (\hat{J}^+\hat{S}^- + \hat{J}^-\hat{S}^+)\}, \tag{6}$$

and another operator, $\hat{\mathscr{H}}^{LU}$, which contains the diagonal terms and the L-uncoupling, off-diagonal terms,

$$\hat{\mathscr{H}}^{LU} = B_{\Lambda,v_\Lambda}\{(\hat{\mathbf{J}}^2 - \hat{J}_z^2) + (\hat{\mathbf{S}}^2 - \hat{S}_z^2) - (\hat{J}^+\hat{L}^- + \hat{J}^-\hat{L}^+)\}. \tag{7}$$

The lifting of the degeneracy described by Eq. (3) is known as Λ-doubling or Λ-splitting. This splitting may be caused by the symmetry dependence of the matrix element in the numerator of Eq. (3) and/or by contributions from different perturbation paths that give rise to a symmetry-dependent energy difference in the denominator. The off-diagonal matrix elements of $\hat{\mathscr{H}}^{Rot}$ and $\hat{\mathscr{H}}^{SO}$ may depend on e/f-symmetry. The off-diagonal matrix elements of $\hat{\mathscr{H}}^{Rot}$ are J-dependent and diagonal in S, whereas the matrix elements of $\hat{\mathscr{H}}^{SO}$ are independent of J and may have off-diagonal contributions in S.

The square of the matrix element in the numerator of Eq. (3) yields three terms, $|\langle i|\hat{\mathscr{H}}^{SO}|j\rangle|^2$, $|\langle i|\hat{\mathscr{H}}^{Rot}|j\rangle|^2$, and $2\langle i|\hat{\mathscr{H}}^{SO}|j\rangle\langle j|\hat{\mathscr{H}}^{Rot}|i\rangle$. A sum over intermediate rotational, vibrational, and electronic states gives rise to the Van Vleck parameters, $o_v(J), p_v(J)$, and $q_v(J)$.[6,7] Here, we simplify the problem by considering only the sum over rotational states.

If we were to ignore the small rotational symmetry dependence of the energy denominator, the Λ-doubling would be determined entirely by the e/f-symmetry of the matrix elements in the numerator. We shall see that the sum of $|\langle i|\hat{\mathscr{H}}^{SO}|j\rangle|^2$ over perturbation paths is independent of e/f-symmetry. It follows that for perturbations with $\Delta S \neq 0$ or for which $\langle i|\hat{\mathscr{H}}^{SO}|j\rangle$ is independent of e/f-symmetry, we would expect the Λ-doubling to be zero. We show in this study that even when the numerator is independent of e/f-symmetry, the symmetry dependence of the energy denominator may produce Λ-doubling.

In the following sections, we present three exemplary cases for which Λ-doubling is produced exclusively by the energy denominator. In Sec. II, we consider the perturbation of a $^1\Pi$ state by a $^3\Sigma^-$ state, for which $\Delta S \neq 0$. In Sec. III, we consider the perturbation of a $^1\Delta$ state by a $^1\Pi$ state, for which $\langle i|\hat{\mathscr{H}}^{Rot}|j\rangle$ is independent of e/f-symmetry. In Sec. IV, we consider the perturbation of a $^2\Pi$ state by a $^4\Sigma^-$. This is a much more complex example of a spin-changing interaction, which involves eight perturbation paths and both Hund's cases (a) and (b) of angular momentum coupling. Finally, in Sec. V, we treat the perturbation of a $^2\Pi$ state by a $^2\Sigma^+$ state, for which both numerator and denominator effects are present. Section VI contains summary and conclusion.

II. SPLITTING OF $^1\Pi$ BY $^3\Sigma^-$

In this section, we treat the example of the perturbation of a $^1\Pi$ state that belongs to a $\pi\sigma$ electronic configuration by a $^3\Sigma^-$ state that belongs to a π^2 configuration. The electronic-rotational wave functions of these states are given by combinations of Slater determinants,[1]

$$\begin{aligned}|^1\Pi_1, J\rangle_{e,f} &= \frac{1}{\sqrt{2}}\left[|^1\Pi_1, v_\Pi\rangle \pm |^1\Pi_{-1}, v_\Pi\rangle\right]\\ &= \frac{1}{2}\big[||\pi^+\alpha, \sigma\beta| - |\pi^+\beta, \sigma\alpha|\rangle|J, 1\rangle\\ &\quad \mp ||\pi^-\beta, \sigma\alpha| - |\pi^-\alpha, \sigma\beta|\rangle|J, -1\rangle\big],\\ |^3\Sigma_1^-, J\rangle_{e,f} &= \frac{1}{\sqrt{2}}\left[|^1\Sigma_1^-, v_\Sigma\rangle \pm |^1\Sigma_{-1}^-, v_\Sigma\rangle\right]\\ &= \frac{1}{\sqrt{2}}[||\pi^+\alpha, \pi^-\alpha|\rangle|J, 1\rangle]\\ &\quad \pm ||\pi^+\beta, \pi^-\beta|\rangle|J, -1\rangle\big],\end{aligned} \tag{8}$$

where the upper sign in each equation corresponds to e-symmetry and the lower sign to f-symmetry.

The perturbation of the $^1\Pi$ state by the $^3\Sigma^-$ state is caused by the spin–orbit term in the Hamiltonian. Applying Eq. (4) to the wave functions in Eq. (8), we obtain for the matrix element in the numerator of Eq. (3) for *both* e- and f-symmetries:

$$\langle ^1\Pi_1, v_\Pi, J|\hat{\mathscr{H}}^{SO}|^3\Sigma_1^-, v_\Sigma, J\rangle = \frac{1}{2\sqrt{2}}\, a_+\langle v_\Pi|v_\Sigma\rangle, \tag{9}$$

where the spin-orbit matrix element for a single spin-orbital[8] is

$$a_+ = \langle\pi^+|\hat{a}\ell^+|\sigma\rangle, \tag{10}$$

and $\langle v_\Pi|v_\Sigma\rangle$ is the vibrational overlap integral.

To evaluate the energy denominator in Eq. (3), we need to calculate the rotational energy levels of the $^3\Sigma^-$ state. These energies are obtained by diagonalizing the spin-uncoupling Hamiltonian. The matrix representation of $\hat{\mathscr{H}}^{SU}$ for this state is

$$\hat{\mathscr{H}}^{SU} = B_{\Sigma,v_\Sigma}\begin{pmatrix} J(J+1) & 2\sqrt{J(J+1)} & 0 \\ 2\sqrt{J(J+1)} & [J(J+1)+2] & 0 \\ 0 & 0 & J(J+1) \end{pmatrix}, \tag{11}$$

where the rows and columns are in the order $^3\Sigma^-_{1,e}$, $^3\Sigma^-_{0,e}$, and $^3\Sigma^-_{1,f}$. The $^3\Sigma^-_0$ state has e-symmetry, and the $^3\Sigma^-_1$ state has pairs of rotational levels of e- and f-symmetry. It is instructive to compare these symmetries with that of the $^3\Sigma^+_0$ state, which has f-symmetry, and those of $^3\Sigma^+_1$, which has pairs of rotational levels of e- and f-symmetry. The eigenvalues of the 2×2, e-block of the Hamiltonian are

$$\begin{aligned} E_+(J) \equiv F_{2e}(J) &= B_{\Sigma,v_\Sigma}(J^2+3J+2), \\ E_-(J) \equiv F_{1e}(J) &= B_{\Sigma,v_\Sigma}(J^2-J), \end{aligned} \tag{12}$$

and the eigenvalue of the 1×1, f-block of the Hamiltonian is

$$E_0(J) \equiv F_{1f}(J) = B_{\Sigma,v_\Sigma}J(J+1). \tag{13}$$

We note that, as expected, the sum of the eigenvalues equals the trace of the matrix.

We introduce a pattern-forming quantum number, N, which has values of $N = J+1$ for E_+, $N = J-1$ for E_-, and $N = J$ for E_0. The energies of levels with a common value of N are

$$\begin{aligned} F_{1e}(N) = E_-(N=J-1) &= B_{\Sigma,v_\Sigma}N(N+1), \\ F_{1f}(N) = E_0(N=J) &= B_{\Sigma,v_\Sigma}N(N+1), \\ F_{2e}(N) = E_+(N=J+1) &= B_{\Sigma,v_\Sigma}N(N+1). \end{aligned} \tag{14}$$

These equations demonstrate why the quantum number N is "pattern-forming."

The rotational levels of the $^3\Sigma^-$ and $^1\Pi$ states are depicted schematically in Fig. 1. The spin-rotational structure of a $^3\Sigma^-$ state consists of sets of three-fold degenerate N-levels, given by Eq. (14). Neighboring sets, with values of the pattern-forming quantum number equal to $N+1$, N, and $N-1$, have the energies

$$\begin{aligned} E(N+1) = E_-(J+2) = E_0(J+1) = E_+(J) \\ = B_{\Sigma,v_\Sigma}(J+1)(J+2), \\ E(N) = E_-(J+1) = E_0(J) = E_+(J-1) = B_{\Sigma,v_\Sigma}J(J+1), \\ E(N-1) = E_-(J) = E_0(J-1) = E_+(J-2) = B_{\Sigma,v_\Sigma}(J-1)J, \end{aligned} \tag{15}$$

which are expressed as functions of the rigorously good quantum number, J. The spacings between these sets, which are shown in Fig. 1, are $E(N+1)-E(N) = 2B_{\Sigma,v_\Sigma}(J+1)$ and $E(N)-E(N-1) = 2B_{\Sigma,v_\Sigma}J$.

Next, we use second-order perturbation theory to calculate the effects of perturbation of the $^1\Pi$ levels by the $^3\Sigma^-$ state. From Eq. (3), the energy shift is

$$\delta E_\Pi(J) = \frac{|\langle {}^1\Pi_1, v_\Pi|\hat{\mathscr{H}}^{SO}|{}^3\Sigma^-_1, v_\Sigma\rangle|^2}{E_\Pi(J)-E_\Sigma(J)}. \tag{16}$$

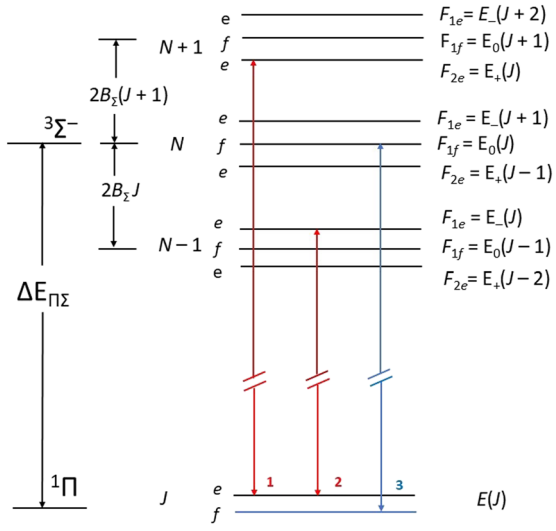

FIG. 1. Rotational energy structure of the $^3\Sigma^-$ and $^1\Pi$ states. The red and blue arrows indicate perturbations of a rotational level, J, of the $^1\Pi$ state by $^3\Sigma^-$ levels of e- and f-symmetry, respectively. The path numbers are indicated at the bottom right of each arrow. Note that for these states, $\Delta E_{\Pi\Sigma}$ is negative.

The numerator of Eq. (16) does not depend on either J or e/f-symmetry, as seen in Eq. (9). The denominator of Eq. (16) is the *symmetry-dependent difference* in energy, $\Delta E_{\Pi\Sigma}$, between the states $|{}^1\Pi_1, v_\Pi, J\rangle$ and $|{}^3\Sigma^-_1, v_\Sigma, J\rangle$. For F_{1f} levels of f-symmetry, this energy difference, depicted by the blue arrow in Fig. 1, is

$$\Delta E_{\Pi\Sigma}(F_{1f}, J) = (T_\Pi - T_\Sigma) + (B_\Pi - B_\Sigma)J(J+1), \tag{17}$$

where T_Π and T_Σ are the electronic term energies of the two states. (Henceforth, for clarity, we drop the v subscript from the rotational constants.) For the F_{1e} and F_{2e} levels of e-symmetry, the energy differences, depicted by the red arrows in Fig. 1, are

$$\begin{aligned} \Delta E_{\Pi\Sigma}(F_{2e}, J) &= \Delta E_{\Pi\Sigma}(F_{1f}, J) - 2B_\Sigma(J+1), \\ \Delta E_{\Pi\Sigma}(F_{1e}, J) &= \Delta E_{\Pi\Sigma}(F_{1f}, J) + 2B_\Sigma J. \end{aligned} \tag{18}$$

The energy shifts of states of e- and f-symmetries are determined by the symmetries of the eigenstates of $\hat{\mathscr{H}}^{SU}$. We express these eigenstates as linear combinations of case (a) basis functions with coefficients c_1, c_2, and c_3, evaluated for the $^3\Sigma^-$ state. By diagonalizing $\hat{\mathscr{H}}^{SU}$, we find that

$$\begin{aligned} |F_{2e}, J\rangle &= c_1(J)\,|{}^3\Sigma^-_1, J\rangle_e + c_2(J)\,|{}^3\Sigma^-_0, J\rangle_e, \\ |F_{1e}, J\rangle &= -c_2(J)\,|{}^3\Sigma^-_1, J\rangle_e + c_1(J)\,|{}^3\Sigma^-_0, J\rangle_e, \\ |F_{1f}, J\rangle &= c_3\,|{}^3\Sigma^-_1, J\rangle_f. \end{aligned} \tag{19}$$

The coefficients of the eigenvectors have the values

$$\begin{aligned} c_1(J) &= \left[\frac{J}{2J+1}\right]^{1/2}, \\ c_2(J) &= \left[\frac{J+1}{2J+1}\right]^{1/2}, \\ c_3 &= 1. \end{aligned} \tag{20}$$

Combining Eqs. (9), (19), and (20), we obtain[9,10]

$$
\begin{aligned}
{}_e\langle {}^3\Sigma_1^-, F_{1e}, J|\hat{\mathscr{H}}^{SO}|{}^1\Pi_1, J\rangle_e &= \left[\frac{J}{2(2J+1)}\right]^{1/2} a_+\langle \mathrm{v}_\Pi|\mathrm{v}_\Sigma\rangle/2,\\
{}_f\langle {}^3\Sigma_1^-, F_{1f}, J|\hat{\mathscr{H}}^{SO}|{}^1\Pi_1, J\rangle_f &= \frac{1}{\sqrt{2}}\, a_+\langle \mathrm{v}_\Pi|\mathrm{v}_\Sigma\rangle/2,\\
{}_e\langle {}^3\Sigma_1^-, F_{2e}, J|\hat{\mathscr{H}}^{SO}|{}^1\Pi_1, J\rangle_e &= -\left[\frac{J+1}{2(2J+1)}\right]^{1/2} a_+\langle \mathrm{v}_\Pi|\mathrm{v}_\Sigma\rangle/2.
\end{aligned}
\tag{21}
$$

Combining Eqs. (16)–(20), we obtain for the energy shift of the state with f-symmetry,

$$
\delta E_{\Pi f}(J) = \frac{\left[{}_f\langle {}^3\Sigma_1^-, F_{1f}, J\hat{\mathscr{H}}^{SO}|{}^1\Pi_1, J\rangle_f\right]^2}{\Delta E_{\Pi\Sigma}(F_{1f}, J)} = \frac{a_+^2\,\langle \mathrm{v}_\Sigma|\mathrm{v}_\Pi\rangle^2}{8\,\Delta E_{\Pi\Sigma}(F_{1f}, J)}. \tag{22}
$$

For e-symmetry, both the F_{1e} and F_{2e} levels contribute to the energy shift. The result is

$$
\begin{aligned}
\delta E_{\Pi e}(J) = &\frac{\left[{}_e\langle {}^3\Sigma_1^-, F_{1e}, J\hat{\mathscr{H}}^{SO}|{}^1\Pi_1, J\rangle_e\right]^2}{\Delta E_{\Pi\Sigma}(F_{1f}, J) - 2B_\Sigma(J+1)}\\
&+ \frac{\left[{}_e\langle {}^3\Sigma_1^-, F_{2e}, J\hat{\mathscr{H}}^{SO}|{}^1\Pi_1, J\rangle_e\right]^2}{\Delta E_{\Pi\Sigma}(F_{1f}, J) + 2B_\Sigma J},
\end{aligned}
\tag{23}
$$

where the energy denominators are defined in Eq. (18). Substituting Eq. (21) into Eq. (23), we obtain

$$
\delta E_{\Pi e}(J) = \frac{a_+^2\langle \mathrm{v}_\Sigma|\mathrm{v}_\Pi\rangle^2}{8\,\Delta E_{\Pi\Sigma}(F_{1f}, J)}\left(\frac{1+2\varepsilon}{1+2\varepsilon-4\varepsilon^2 J(J+1)}\right), \tag{24}
$$

where $\varepsilon \equiv B_\Sigma/\Delta E_{\Pi\Sigma}$. Expanding the denominator to second order in ε, we obtain

$$
\delta E_{\Pi e}(J) \approx \frac{a_+^2\langle \mathrm{v}_\Sigma|\mathrm{v}_\Pi\rangle^2}{8\,\Delta E_{\Pi\Sigma}(F_{1f}, J)}\left\{1+4\varepsilon^2 J(J+1)\right\}. \tag{25}
$$

We obtain, finally, for the Λ-splitting,

$$
\begin{aligned}
\delta\nu({}^1\Pi \sim {}^3\Sigma^-, J) &= [\delta E_{\Pi f}(J) - \delta E_{\Pi e}(J)]/h\\
&= -\frac{a_+^2 B_\Sigma^2\langle \mathrm{v}_\Sigma|\mathrm{v}_\Pi\rangle^2}{2h\left[\Delta E_{\Pi\Sigma}(F_{1f}, J)\right]^3}\, J(J+1).
\end{aligned}
\tag{26}
$$

It is insightful to compare this result to the direct splitting of ${}^1\Pi$ by ${}^1\Sigma$ states. The matrix elements in the numerator are

$$
\begin{aligned}
B_{\mathrm{v}_\Pi,\mathrm{v}_\Sigma}\langle {}^1\Pi_e, J|\hat{J}^+\hat{L}^-|{}^1\Sigma_e^+, J\rangle &= B_{\mathrm{v}_\Pi,\mathrm{v}_\Sigma}\langle {}^1\Pi_f, J|\hat{J}^+\hat{L}^-|{}^1\Sigma_f^-, J\rangle\\
&= B_{\mathrm{v}_\Pi,\mathrm{v}_\Sigma} b_{\Pi\Sigma}\sqrt{J(J+1)},
\end{aligned}
\tag{27}
$$

where $b_{\Pi\Sigma} = \langle\Sigma|\hat{L}^-|\Pi\rangle$ is a rotation-orbit or gyroscopic parameter. In this case, there is only *one* perturbation path. Either the ${}^1\Pi_e$ state is perturbed by a ${}^1\Sigma_e^+$ state and the energy of the ${}^1\Pi_f$ state is not shifted, or the ${}^1\Pi_f$ state is perturbed by a ${}^1\Sigma_f^-$ state and the energy of the ${}^1\Pi_e$ state is not shifted. The Λ doubling in this case is

$$
\delta\nu({}^1\Pi \sim {}^1\Sigma^\pm, J) = \mp\frac{B_\Sigma^2\, b_{\Pi\Sigma}^2\langle \mathrm{v}_\Sigma|\mathrm{v}_\Pi\rangle^2}{h\Delta\left[E_{\Pi\Sigma}(F_{1f}, J)\right]}\, J(J+1). \tag{28}
$$

It follows that the ratio of the Λ-splitting by the denominator effect in Eq. (26) to the splitting by the numerator in Eq. (28) is

$$
\frac{\delta\nu\left({}^1\Pi \sim {}^3\Sigma^-, J\right)}{\delta\nu\left({}^1\Pi \sim {}^1\Sigma^\pm, J\right)} = \pm\frac{1}{2}\left(\frac{a_+}{\Delta E_{\Pi\Sigma}}\right)^2\left(\frac{\langle \mathrm{v}_\Sigma|\mathrm{v}_\Pi\rangle}{b_{\Pi\Sigma}}\right)^2. \tag{29}
$$

A perturbing state is said to be "energetically remote" when $a_+ \ll \Delta E$, in which case, the ratio of the two splttings in Eq. (29) is very small.

III. SPLITTING OF ${}^1\Delta$ BY ${}^1\Pi$

For the perturbation of ${}^1\Delta$ by ${}^1\Pi$ states, the off-diagonal matrix element of $\hat{\mathscr{H}}^{Rot}$ is independent of e/f-symmetry. In this case, the second-order Λ-splitting of the ${}^1\Pi$ state produces a fourth-order splitting of the ${}^1\Delta$ state.

The wave functions of the ${}^1\Pi$ and ${}^1\Delta$ states are

$$
\begin{aligned}
|{}^1\Pi_1, J\rangle_{e,f} &= \frac{1}{\sqrt{2}}\left\{|{}^1\Pi_1\rangle|J, 1\rangle \pm |{}^1\Pi_{-1}\rangle|J, -1\rangle\right\},\\
|{}^1\Delta_2, J\rangle_{e,f} &= \frac{1}{\sqrt{2}}\left\{|{}^1\Delta_2\rangle|J, 2\rangle \pm |{}^1\Delta_{-2}\rangle|J, -2\rangle\right\},
\end{aligned}
\tag{30}
$$

and the matrix element in the numerator of the perturbation equation, $\delta\nu = |\langle i|\hat{V}|j\rangle|^2/h\Delta E_{ij}$, is

$$
\langle {}^1\Pi_1|\hat{\mathscr{H}}^{LU}|{}^1\Delta_2\rangle = \frac{1}{\sqrt{2}}\, b_{\Pi\Delta} B_{\mathrm{v}_\Pi,\mathrm{v}_\Delta}\,[J(J+1)-2]^{\frac{1}{2}}. \tag{31}
$$

It is apparent from Eq. (30) that this matrix element has the same value for e- and f-symmetries. The denominator, however, depends on e/f symmetry owing to the splitting of the ${}^1\Pi$ state by the ${}^3\Sigma$ state, which was derived in Sec. II. The resulting energy shifts for e- and f-symmetry are

$$
\begin{aligned}
\delta E_e(J) &= \frac{\frac{1}{2}\, b_{\Pi\Delta}^2\, B_{\mathrm{v}_\Pi,\mathrm{v}_\Delta}^2[J(J+1)-2]}{\Delta E_{\Pi\Delta} + \delta_\Pi(J)/2},\\
\delta E_f(J) &= \frac{\frac{1}{2}\, b_{\Pi\Delta}^2\, B_{\mathrm{v}_\Pi,\mathrm{v}_\Delta}^2[J(J+1)-2]}{\Delta E_{\Pi\Delta} - \delta_\Pi(J)/2}.
\end{aligned}
\tag{32}
$$

After some algebra, the Λ-splitting of the ${}^1\Delta$ state is found to be

$$
\begin{aligned}
\delta\nu_\Delta(J) &= [\delta E_{\Delta f}(J) - \delta E_{\Delta e}(J)]/h\\
&= -\frac{b_{\Pi\Delta}^2\, B_{\mathrm{v}_\Pi,\mathrm{v}_\Delta}^2[J(J+1)-2]}{2\left(\Delta E_{\Pi\Delta}\right)^2}\,\delta\nu_\Pi(J).
\end{aligned}
\tag{33}
$$

Comparing this result to Eq. (26), we see that, whereas $\delta\nu_\Pi(J)$ varies as J squared, $\delta\nu_\Delta(J)$ varies as J to the fourth power, which corresponds to a fourth-order perturbation. This result is consistent with the result derived for direct (numerator) Λ-doubling of Δ states by Brown *et al.*,[11] and in references cited therein.

IV. SPLITTING OF ${}^2\Pi$ BY ${}^4\Sigma^-$

A. Introduction

The Λ-doubling of a ${}^2\Pi$ state by an energetically remote ${}^4\Sigma^-$ state is another example where the interaction is caused exclusively

by the spin–orbit operator and the splitting is exclusively a denominator effect. This case is complicated by the multiplet structure of the $^4\Sigma^-$ state and by the angular momentum coupling of the $^2\Pi$ state.

In calculating the Λ-doubling, the following points are considered. First, the spin-orbit selection rule, $\Delta\Omega = 0$, requires that the only possible interactions are $^2\Pi_{\frac{1}{2}} \sim {}^4\Sigma^-_{\frac{1}{2}}$ and $^2\Pi_{\frac{3}{2}} \sim {}^4\Sigma^-_{\frac{3}{2}}$. Second, in the absence of a perturbation, the $^4\Sigma^-$ state is four-fold degenerate. It is necessary to identify the e/f-symmetry of each of the four degenerate states and to specify the perturbation paths for $^2\Pi$ states of the same J and e/f-symmetry. Third, to calculate the interaction of the $^2\Pi$ state with each of the $^4\Sigma^-$ multiplet components, it is necessary to take into account the angular momentum coupling of the $^2\Pi$ state. Here we consider the perturbation near the Hund's case (a) and case (b) limits of the $^2\Pi$ state.

B. Properties of the $^4\Sigma$ states

The spin-uncoupling rotational Hamiltonian is given by Eq. (6). The matrix representation of this operator for the $^4\Sigma^-$ state with e-symmetry in the case (a) basis is

$$\langle\psi_i|\hat{\mathscr{H}}^{SU}|\psi_j\rangle = B_\Sigma\begin{pmatrix} J(J+1)-3/4 & [3(J-1/2)(J+3/2)]^{\frac{1}{2}} \\ [3(J-1/2)(J+3/2)]^{\frac{1}{2}} & J(J+1)-2J+9/4 \end{pmatrix}, \tag{34}$$

where the rows and columns are in the order $^4\Sigma^-_{\frac{3}{2}}, {}^4\Sigma^-_{\frac{1}{2}}$. We diagonalize the matrix and solve for the roots of the secular equation. The results are

$$\begin{aligned} E_{e+} &= B_\Sigma(J^2+2J+3/4), \\ E_{e-} &= B_\Sigma(J^2-2J+3/4). \end{aligned} \tag{35}$$

Similarly, the matrix representation of $\hat{\mathscr{H}}^{SU}$ for the $^4\Sigma^-$ state with f-symmetry is

$$\langle\psi_i|\hat{\mathscr{H}}^{SU}|\psi_j\rangle = B_\Sigma\begin{pmatrix} J(J+1)-3/4 & [3(J-1/2)(J+3/2)]^{\frac{1}{2}} \\ [3(J-1/2)(J+3/2)]^{\frac{1}{2}} & J(J+1)+2J+17/4 \end{pmatrix}, \tag{36}$$

and its roots are

$$\begin{aligned} E_{f+} &= B_\Sigma(J^2+4J+15/4), \\ E_{f-} &= B_\Sigma(J^2-1/4). \end{aligned} \tag{37}$$

We label the states in the order of increasing energy for a given e- or f-symmetry and a fixed value of J. The states with energies E_{e-}, E_{e+}, E_{f-}, and E_{f+} are labeled F_{1e}, F_{2e}, F_{1f}, and F_{2f}, respectively.[13] We define the pattern-forming quantum number, N, such that

$$\begin{aligned} N &= J-3/2, \quad F_{1e}, \\ N &= J+1/2, \quad F_{2e}, \\ N &= J-1/2, \quad F_{1f}, \\ N &= J+3/2, \quad F_{2f}. \end{aligned} \tag{38}$$

After substituting Eq. (38) into Eqs. (35) and (37), we find that the energies of all four levels are given by

$$E(N) = B_\Sigma N(N+1), \tag{39}$$

which reflects the pattern-forming nature of N in case (b).

We note that case (b) coupling is suitable for $^4\Sigma^-$ states at all values of J. We also note that interchanging $^4\Sigma^-$ with $^4\Sigma^+$ is equivalent to interchanging e- and f-symmetries. We may see this by comparing the H_{22} matrix elements in Eqs. (34) and (36). The relevant wave functions are

$$\begin{aligned} |{}^4\Sigma^+_{\frac{1}{2}}, J\rangle_e &= 2^{-\frac{1}{2}}\left[|{}^4\Sigma^+_{\frac{1}{2}}\rangle|J,1/2\rangle\right] + |{}^4\Sigma^+_{-\frac{1}{2}}\rangle|J,-1/2\rangle\Big], \\ |{}^4\Sigma^-_{\frac{1}{2}}, J\rangle_f &= 2^{-\frac{1}{2}}\left[|{}^4\Sigma^-_{\frac{1}{2}}\rangle|J,1/2\rangle\right] + |{}^4\Sigma^-_{-\frac{1}{2}}\rangle|J,-1/2\rangle\Big]. \end{aligned} \tag{40}$$

The plus sign in the sum for both wave functions is derived from Eq. (3.2.94) in Ref. 1. The $\Omega = \Omega' = 1/2$ matrix element for both states is

$$\begin{aligned} H_{22} &= B_\Sigma\left[J(J+1) - 2\left(\frac{1}{2}\right)\left(\frac{1}{2}\right) + \frac{15}{4} + \underline{(2J+1)}\right] \\ &= B_\Sigma[J(J+1)+2J+17/4], \end{aligned} \tag{41}$$

where the underlined term comes from $\hat{J}^+\hat{S}^- + \hat{J}^-\hat{S}^+$. Similarly,

$$\begin{aligned} |{}^4\Sigma^+_{\frac{1}{2}}, J\rangle_f &= 2^{-\frac{1}{2}}\left[|{}^4\Sigma^+_{\frac{1}{2}}\rangle|J,1/2\rangle\right] - |{}^4\Sigma^+_{-\frac{1}{2}}\rangle|J,-1/2\rangle\Big], \\ |{}^4\Sigma^+_{\frac{1}{2}}, J\rangle_e &= 2^{-\frac{1}{2}}\left[|{}^4\Sigma^-_{\frac{1}{2}}\rangle|J,1/2\rangle\right] - |{}^4\Sigma^-_{-\frac{1}{2}}\rangle|J,-1/2\rangle\Big], \end{aligned} \tag{42}$$

and

$$\begin{aligned} H_{22} &= B_\Sigma\left[J(J+1) - 2\left(\frac{1}{2}\right)\left(\frac{1}{2}\right) + \frac{15}{4} - \underline{(2J+1)}\right], \\ &= B_\Sigma[J(J+1)-2J+9/4]. \end{aligned} \tag{43}$$

It follows that the matrix representations of $\hat{\mathscr{H}}^{SU}$ for $^4\Sigma^\mp_e$ and $^4\Sigma^\pm_f$ are equivalent.

We next derive the wave function associated with each energy eigenstate by solving the following equation:

$$\hat{\mathscr{H}}^{SU}|{}^4\Sigma^-, F_k, J\rangle = E_k|{}^4\Sigma^-, F_k, J\rangle, \qquad k = 1, 2. \tag{44}$$

The results for $^4\Sigma^-$ states with e-symmetry and the corresponding results for $^4\Sigma^+$ states with f-symmetry are

$$\begin{aligned} |{}^4\Sigma^-, F_1, J\rangle_e &= \left(\frac{3(J-1/2)}{4J}\right)^{\frac{1}{2}} |{}^4\Sigma^-_{\frac{1}{2}}, J\rangle_e + \left(\frac{J+3/2}{4J}\right)^{\frac{1}{2}} |{}^4\Sigma^-_{\frac{3}{2}}, J\rangle_e, \\ |{}^4\Sigma^-, F_2, J\rangle_e &= \left(\frac{J+3/2}{4J}\right)^{\frac{1}{2}} |{}^4\Sigma^-_{\frac{1}{2}}, J\rangle_e - \left(\frac{3(J-1/2)}{4J}\right)^{\frac{1}{2}} |{}^4\Sigma^-_{\frac{3}{2}}, J\rangle_e, \end{aligned} \tag{45}$$

where

$$\begin{aligned} |{}^4\Sigma^-_{\frac{1}{2}}, J\rangle_e &= 2^{-\frac{1}{2}}\left\{|{}^4\Sigma^-_{\frac{1}{2}}\rangle|J,1/2\rangle + |{}^4\Sigma^-_{-\frac{1}{2}}\rangle|J,-1/2\rangle\right\}, \\ |{}^4\Sigma^-_{\frac{3}{2}}, J\rangle_e &= 2^{-\frac{1}{2}}\left\{|{}^4\Sigma^-_{\frac{3}{2}}\rangle|J,3/2\rangle + |{}^4\Sigma^-_{-\frac{3}{2}}\rangle|J,-3/2\rangle\right\}. \end{aligned} \tag{46}$$

Similarly, the results for $^4\Sigma^-$ states with f-symmetry (and the corresponding results for $^4\Sigma^+$ states with e-symmetry) are

$$|^4\Sigma^-, F_1, J\rangle_f = \left(\frac{3(J+3/2)}{4(J+1)}\right)^{\frac{1}{2}} |^4\Sigma^-_{\frac{1}{2}}, J\rangle_f + \left(\frac{J-1/2}{4(J+1)}\right)^{\frac{1}{2}} |^4\Sigma^-_{\frac{3}{2}}, J\rangle_f,$$
$$|^4\Sigma^-, F_2, J\rangle_f = \left(\frac{J-1/2}{4(J+1)}\right)^{\frac{1}{2}} |^4\Sigma^-_{\frac{1}{2}}, J\rangle_f - \left(\frac{3(J+3/2)}{4(J+1)}\right)^{\frac{1}{2}} |^4\Sigma^-_{\frac{3}{2}}, J\rangle_f, \quad (47)$$

where

$$|^4\Sigma^-_{\frac{1}{2}}, J\rangle_f = 2^{-\frac{1}{2}}\left\{|^4\Sigma^-_{\frac{1}{2}}\rangle|J, 1/2\rangle - |^4\Sigma^-_{-\frac{1}{2}}\rangle|J, -1/2\rangle\right\},$$
$$|^4\Sigma^-_{\frac{3}{2}}, J\rangle_f = 2^{-\frac{1}{2}}\left\{|^4\Sigma^-_{\frac{3}{2}}\rangle|J, 3/2\rangle - |^4\Sigma^-_{-\frac{3}{2}}\rangle|J, -3/2\rangle\right\}. \quad (48)$$

It will be convenient when describing the perturbation paths to refer to the eigenfunctions in Eqs. (45) and (47) as the e_1, e_2, f_1, and f_2 eigenstates associated with the $^4\Sigma^-$ state.

C. Properties of the $^2\Pi$ state

Unlike the $^4\Sigma^\pm$ states, the angular coupling of $^2\Pi$ evolves from case (a) toward case (b) with increasing J. Here, we consider the limits of pure case (a) and pure case (b).

In the case (a) limit, the $^2\Pi$ state functions are

$$|^2\Pi_{\frac{3}{2}}, J\rangle_{e/f} = 2^{-\frac{1}{2}}\left[|^2\Pi_{\frac{3}{2}}\rangle|J, 3/2\rangle \pm |^2\Pi_{-\frac{3}{2}}\rangle|J, -3/2\rangle\right],$$
$$|^2\Pi_{\frac{1}{2}}, J\rangle_{e/f} = 2^{-\frac{1}{2}}\left[|^2\Pi_{\frac{1}{2}}\rangle|J, 1/2\rangle \pm |^2\Pi_{-\frac{1}{2}}\rangle|J, -1/2\rangle\right]. \quad (49)$$

The case (b) $^2\Pi$ wave functions are expanded in the case (a) basis by means of a unitary transformation,

$$|J, S, N, \Lambda\rangle = \sum_{\Sigma=-S}^{S} (J, \Omega, S, -\Sigma|J, S, N, \Lambda)|J, \Omega, S, \Sigma\rangle, \quad (50)$$

where the quantity in parentheses is a Clebsch–Gordan coefficient, and it is understood that $\Lambda = \Omega - \Sigma$. (See p. 130 in Ref. 1.) For a $^2\Pi$ state,

$$|^2\Pi, F_1, N = J - 1/2\rangle_{e/f} = \left(\frac{J-1/2}{2J+1}\right)^{1/2} |^2\Pi_{1/2}\rangle_{e/f} + \left(\frac{J+3/2}{2J+1}\right)^{1/2} |^2\Pi_{3/2}\rangle_{e/f},$$
$$|^2\Pi, F_2, N = J + 1/2\rangle_{e/f} = \left(\frac{J+3/2}{2J+1}\right)^{1/2} |^2\Pi_{1/2}\rangle_{e/f} - \left(\frac{J-1/2}{2J+1}\right)^{1/2} |^2\Pi_{3/2}\rangle_{e/f}. \quad (51)$$

It will be convenient to refer to these functions as the e_1, e_2, f_1, and f_2 eigenstates associated with the $^2\Pi$ state. We use the symbol N_0 to designate the pattern forming quantum number and the symbol $J_0 = J$ for the total angular momentum quantum number of the $^2\Pi$ state, so that the relations between J and N introduced in Eq. (51) are

$$N_0 = J_0 + 1/2, \quad F_{2e}, F_{2f},$$
$$N_0 = J_0 - 1/2, \quad F_{1e}.F_{1f}. \quad (52)$$

D. Matrix elements for each of the perturbation paths

We use the results of the previous sections to evaluate the matrix elements that appear in the numerator of the second-order perturbation theory expression [Eq. (16)] for the energy shift. We evaluate these matrix elements in the case (a) and case (b) limits. Since there are four eigenstates for $^2\Pi$ and $^4\Sigma^-$, there are 16 matrix elements to be considered in each limit. Conservation of symmetry (i.e., the requirement that e-states perturb only e-states and f-states perturb only f-states) reduces this number to 8. These interactions are shown schematically[12] in Fig. 2 for case (a), and the corresponding perturbation paths are depicted in Fig. 3.

The paths that connect rotational levels of $^2\Pi$ and $^4\Sigma^-$ must conserve e/f symmetry and the total angular momentum quantum number, J. The quantum numbers of the $^4\Sigma^-$ state, which are listed to the right of the energy levels in Fig. 3, are determined by invoking the relation between N and J given in Eq. (38). For example, $J = N - 3/2$ for all four f_2 levels shown in this figure. Path 4 connects the f_2 level of $^2\Pi(F_2, J_0)$ with the f_2 level of $^4\Sigma^-(N = J_0 + 3/2)$. Following the same reasoning, path 3 connects the same f_2 level of $^2\Pi(F_2, J_0)$ with the f_1 level of $^4\Sigma^-(N = J_0 - 1/2)$. We refer to path 4 by the label $f_2 - f_2$ and path 3 by the label $f_2 - f_1$. The other paths are named similarly.

Similar reasoning is applied in the case (b) limit of $^2\Pi$, except that in this case, N is a pattern forming quantum number, and the selection rule $\Delta N = 0, \pm 1$ applies. We denote the corresponding quantum number for the $^2\Pi$ state by N_0. Figure 4 shows that paths (2) and (8), which involve $\Delta N = \pm 2$, are not allowed. The corresponding path diagram is given by Fig. 5.

It is instructive to use Eqs. (35) and (37) to calculate the energy levels depicted in Fig. 5. The four $^4\Sigma^-$ levels associated with each value of N are degenerate. For example, the levels with $N = N_0$ all have a rotational energy of $B_\Sigma N_0(N_0 + 1)$. For the e_1 level, Eqs. (35) and (38) give $J = N_0 + 3/2$ and

$$E(^4\Sigma^-, J, e_1) = B_\Sigma(J^2 - 2J + 3/4) = B_\Sigma N_0(N_0 + 1). \quad (53)$$

The same result is obtained for $E(^4\Sigma^-, J, f_1), E(^4\Sigma^-, J, e_2)$ and $E(^4\Sigma^-, J, f_2)$.

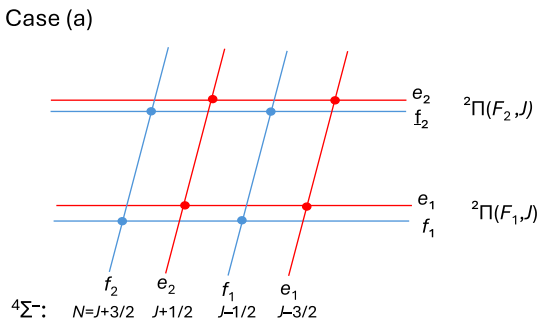

FIG. 2. Schematic diagram of the spin–orbit interactions of the rotational levels of the $^2\Pi$ and $^4\Sigma^-$ states in the case (a) limit of the $^2\Pi$ state. This diagram shows that $^4\Sigma^-$ states of e- or f-symmetry interact only with $^2\Pi$ states of the same e/f symmetry. The red lines and dots correspond to e-symmetry, and the blue ones correspond to f-symmetry.

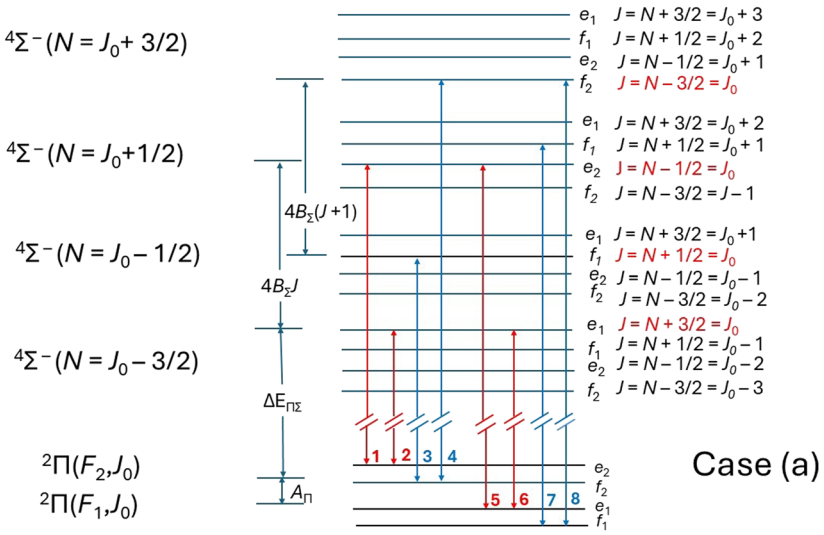

FIG. 3. Diagram of the rotational energy levels of the $^2\Pi$ and $^4\Sigma^-$ states in the case (a) limit of the $^2\Pi$ state. The arrows indicate the symmetry-allowed paths for spin–orbit interactions. The path numbers are indicated at the bottom right of each arrow. Paths 1, 2, 5, and 6—shown in red—indicate the interactions of states of *e*-symmetry, and paths 3, 4, 7, and 8—shown in blue—indicate the interactions of states of *f*-symmetry. In each of the contributing interactions, $J = J_0$, as indicated by the red annotation on the right side of the figure. The separations between the *e*- and *f*-energy levels are calculated using Eqs. (35) and (37). Note that for these states, $\Delta E_{\Pi\Sigma}$ is negative.

Similarly, the four levels associated with the $^2\Pi$ state in case (b) are degenerate. Diagonalization of $\hat{\mathscr{H}}^{SU}$ yields[7,14]

$$E_\pm = B_\Pi\left[(J+1/2)^2 - \Lambda^2 \pm X_v/2\right], \tag{54}$$

where

$$X_v = \left[Y_v(Y_v - 4) + 4(J+1/2)^2\right]^{\frac{1}{2}}, \quad Y_v = A_\Pi/B_\Pi. \tag{55}$$

The plus sign in Eq. (54) corresponds to e_2 and f_2, and the minus sign corresponds to e_1 and f_1. For $Y_v = 0$ or 4, we obtain $X_v/2 = J + 1/2$. Inserting the relations between N_0 and J_0 given by Eq. (52) and setting $\Lambda = 1$ for a Π state, we obtain the energy for both *e*- and *f*-symmetries in case (b):

$$E = B_\Pi[N_0(N_0+1) - 1]. \tag{56}$$

We now have all the tools needed to calculate the off-diagonal matrix elements of $\hat{\mathscr{H}}^{SO}$ for each path. The results are listed in Table I of the Appendix. The path numbers correspond to those in Figs. 3 and 5. The paths are labeled $s_i - s'_j$, where s is the e/f symmetry of the $^2\Pi$ level, s' is the e/f symmetry of the $^4\Sigma^-$ level, and i and j each equal 1 or 2. We label the matrix elements $c_{1a}, \ldots, c_{8a}$ for Hund's case (a) and $c_{1b}, \ldots, c_{8b}$ for Hund's case (b). A property of these coefficients is that the sum of their squares for a given *e*- or *f*-symmetry is independent of symmetry. For example, $c_{1a}^2 + c_{2a}^2 = c_{3a}^2 + c_{4a}^2$. This property is important because it implies that even though the off-diagonal matrix elements of $\hat{\mathscr{H}}^{SO}$ may depend on e/f-symmetry, the square of these matrix elements summed over all paths belonging to a particular perturbation [in this case, paths 1 and 2 for $^2\Pi(F_{2e},J) \sim {}^4\Sigma^-(J,e)$ and paths 3 and 4 for $^2\Pi(F_{2f},J) \sim {}^4\Sigma^-(J,f)$] is the same for both symmetries. [The same property is shown in Eq. (20) for $^1\Pi \sim {}^3\Sigma^-$.] It follows that if $\hat{\mathscr{H}}^{Rot}$ does not introduce e/f-symmetry dependence of the numerator (in this case because $\Delta S \neq 0$), the only source of Λ-doubling is the energy denominator.

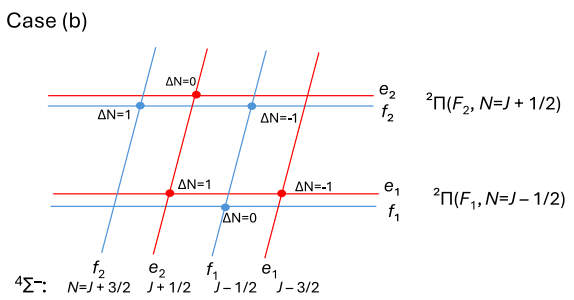

FIG. 4. Schematic diagram of the spin–orbit interactions of the rotational levels of the $^2\Pi$ and $^4\Sigma^-$ states in the case (b) limit of the $^2\Pi$ state. The red lines and dots correspond to *e*-symmetry, and the blue ones correspond to *f*-symmetry. The labeled dots indicate the $\Delta N = 0, \pm 1$ selection rule for the matrix elements. This diagram is a revised version of Fig. 4.69 in Ref. 9.

E. Calculation of the Λ-doubling: Case (a)

We use the matrix elements listed in Table I to calculate the Λ-doubling. We consider first the case (a) limit of the $^2\Pi$ state. For the F_2 state (i.e., for $^2\Pi_{3/2}$ with $A_\Pi > 0$ and $^2\Pi_{1/2}$ with $A_\Pi < 0$), the energy shift of the *e*-levels is the sum of the contributions from paths 1 and 2. The energy denominator is calculated using Eq. (35), which gives, for these two paths, $E(^4\Sigma^-, J_0, e_2) - E(^4\Sigma^-, J_0, e_1) = 4B_\Sigma J_0$. The energy shift from the two paths is

$$\begin{aligned}\delta E_{\Pi(F_2,e)} &= \frac{c_{1a}^2}{\Delta E_{\Pi\Sigma} - 4B_\Sigma J_0} + \frac{c_{2a}^2}{\Delta E_{\Pi\Sigma}} = \frac{1}{4}a_+^2\langle v_\Pi | v_\Sigma\rangle^2 \\ &\times \left\{\frac{3}{4}\left(\frac{J_0 - 1/2}{J_0}\right)\frac{1}{\Delta E_{\Pi\Sigma} - 4B_\Sigma J_0} + \frac{1}{4}\left(\frac{J_0 + 3/2}{J_0}\right)\frac{1}{\Delta E_{\Pi\Sigma}}\right\} \\ &= \frac{a_+^2\langle v_\Pi | v_\Sigma\rangle^2}{4\Delta E_{\Pi\Sigma}}\left\{\frac{3}{4}\left(\frac{J_0 - 1/2}{J_0}\right)\frac{1}{1 - 4\varepsilon J_0} + \frac{1}{4}\left(\frac{J_0 + 3/2}{J_0}\right)\right\} \\ &\approx \frac{a_+^2\langle v_\Pi | v_\Sigma\rangle^2}{4\Delta E_{\Pi\Sigma}}[1 + 3\varepsilon(J_0 - 1/2)],\end{aligned} \tag{57}$$

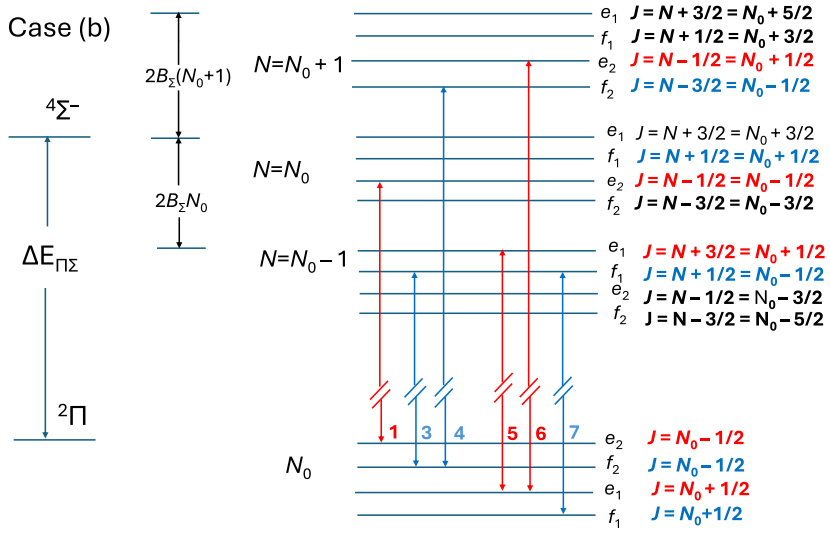

FIG. 5. Diagram of the rotational energy levels of the $^2\Pi$ and $^4\Sigma^-$ states in the case (b) limit of the $^2\Pi$ state. The arrows indicate the symmetry-allowed paths for spin–orbit interactions. The path numbers are indicated at the bottom right of each arrow. Paths 1, 5, and 6—shown in red—indicate the interactions of states of *e*-symmetry, and paths 3, 4, and 7—shown in blue—indicate the interactions of states of *f*-symmetry.

TABLE I. Matrix elements for the perturbation paths connecting the $^2\Pi$ and $^4\Sigma^-$ states.[a]

Path	$\langle {}^2\Pi(a), J\vert\hat{\mathscr{H}}^{SO}\vert {}^4\Sigma^-, J\rangle$	$\langle {}^2\Pi(b), J\vert\hat{\mathscr{H}}^{SO}\vert {}^4\Sigma^-, J\rangle$	$\langle {}^2\Pi(b), N_0\vert\hat{\mathscr{H}}^{SO}\vert {}^4\Sigma^-, N_0\rangle$
(1) $e_2 - e_2$	$-\sqrt{\frac{3}{4}}\sqrt{\frac{J-1/2}{J}}$	$-\sqrt{\frac{2}{3}}\sqrt{\frac{J}{J+1/2}}$	$-\sqrt{\frac{2}{3}}\sqrt{\frac{N_0-1/2}{N_0}}$
(2) $e_2 - e_1$	$-\frac{1}{2}\sqrt{\frac{J+3/2}{J}}$	0	0
(3) $f_2 - f_1$	$-\sqrt{\frac{3}{4}}\sqrt{\frac{J+3/2}{J+1}}$	$\sqrt{\frac{1}{6}}\sqrt{\frac{(J-1/2)(J+3/2)}{(J+1/2)(J+1)}}$	$\sqrt{\frac{1}{6}}\sqrt{\frac{N_0^2-1}{N_0(N_0+1/2)}}$
(4) $f_2 - f_2$	$-\frac{1}{2}\sqrt{\frac{J-1/2}{J+1}}$	$\sqrt{\frac{1}{2}}\sqrt{\frac{J+1/2}{J+1}}$	$\sqrt{\frac{1}{2}}\sqrt{\frac{N_0}{N_0+1/2}}$
(5) $e_1 - e_2$	$-\sqrt{\frac{1}{12}}\sqrt{\frac{J+3/2}{J}}$	$\sqrt{\frac{1}{6}}\sqrt{\frac{(J-1/2)(J+3/2)}{J(J+1/2)}}$	$\sqrt{\frac{1}{6}}\sqrt{\frac{N_0(N_0+2)}{(N_0+1/2)(N_0+1)}}$
(6) $e_1 - e_1$	$-\frac{1}{2}\sqrt{\frac{J-1/2}{J}}$	$-\sqrt{\frac{1}{2}}\sqrt{\frac{J+1/2}{J}}$	$-\sqrt{\frac{1}{2}}\sqrt{\frac{N_0+1}{N_0+1/2}}$
(7) $f_1 - f_1$	$-\sqrt{\frac{1}{12}}\sqrt{\frac{J-1/2}{J+1}}$	$-\sqrt{\frac{2}{3}}\sqrt{\frac{J+1}{J+1/2}}$	$-\sqrt{\frac{2}{3}}\sqrt{\frac{N_0+3/2}{N_0+1}}$
(8) $f_1 - f_2$	$\frac{1}{2}\sqrt{\frac{J+3/2}{J+1}}$	0	0

[a]The matrix elements are divided by a common factor of $a_+\langle \mathrm{v}_\Pi\vert\mathrm{v}_\Sigma\rangle/2$.

where

$$\Delta E_{\Pi\Sigma}(F_2, J) = (T_\Pi - T_\Sigma) + (B_\Pi - B_\Sigma)J_0(J_0+1), \tag{58}$$

and $\varepsilon = B_\Sigma/\Delta E_{\Pi\Sigma}$.

Similarly, the energy shift of the *f*-levels is produced by paths 3 and 4. The energy denominators are calculated from Eqs. (35) and (37), which give

$$\begin{aligned} E(^4\Sigma^-, J_0, f_1) - E(^4\Sigma^-, J_0, e_1) &= 2B_\Sigma(J_0 - 1/2), \\ E(^4\Sigma^-, J_0, f_2) - E(^4\Sigma^-, J_0, e_1 &= 6B_\Sigma(J_0 + 1/2) \end{aligned} \tag{59}$$

The resulting energy shift is

$$\begin{aligned} \delta E_{\Pi(F_2,f)} &= \frac{c_{3a}^2}{\Delta E_{\Pi\Sigma} - 2B_\Sigma(J_0 - 1/2)} + \frac{c_{4a}^2}{\Delta E_{\Pi\Sigma} - 6B_\Sigma(J_0 + 1/2)} \\ &= \frac{a_+^2\langle \mathrm{v}_\Pi\vert\mathrm{v}_\Sigma\rangle^2}{4\Delta E_{\Pi\Sigma}}\left\{\frac{3}{4}\left(\frac{J_0+3/2}{J_0+1}\right)\frac{1}{1-2\varepsilon(J_0-1/2)}\right. \\ &\quad \left. + \frac{1}{4}\left(\frac{J_0-1/2}{J_0+1}\right)\frac{1}{1-6\varepsilon(J_0+1/2)}\right\} \\ &\approx \frac{a_+^2\langle \mathrm{v}_\Pi\vert\mathrm{v}_\Sigma\rangle^2}{4\Delta E_{\Pi\Sigma}}\left\{\frac{3}{4}\left(\frac{J_0+3/2}{J_0+1}\right)[1+2\varepsilon(J_0-1/2)]\right. \\ &\quad \left. + \frac{1}{4}\left(\frac{J_0-1/2}{J_0+1}\right)[1+6\varepsilon(J_0+1/2)]\right\} \\ &= \frac{a_+^2\langle \mathrm{v}_\Pi\vert\mathrm{v}_\Sigma\rangle^2}{4\Delta E_{\Pi\Sigma}}[1+3\varepsilon(J_0-1/2]. \end{aligned} \tag{60}$$

Comparison of Eqs. (57) and (60) shows that the denominators do not generate Λ-doubling of the F_2 levels.

We perform a similar calculation of the splitting of the F_1 levels of the $^2\Pi$ state. For paths 5 and 6, the relevant energy difference, calculated using Eq. (35), is $E(^4\Sigma^-, e_2) - E(^4\Sigma^-, e_1) = 4B_\Sigma J_0$. The energy shift of the e-level is

$$\begin{aligned}\delta E_{\Pi(F_2,e)} &= \frac{c_{5a}^2}{\Delta E_{\Pi\Sigma} + A_\Pi - 4B_\Sigma J_0} + \frac{c_{6a}^2}{\Delta E_{\Pi\Sigma} + A_\Pi} \\ &= \frac{1}{4} a_+^2 \langle v_\Pi | v_\Sigma \rangle^2 \left\{ \frac{1}{12} \left(\frac{J_0 + 3/2}{J_0} \right) \frac{1}{\Delta E_{\Pi\Sigma} + A_\Pi - 4B_v J_0} \right. \\ &\quad \left. + \frac{1}{4} \left(\frac{J_0 - 1/2}{J_0} \right) \frac{1}{\Delta E_{\Pi\Sigma} + A_\Pi} \right\} \\ &= \frac{1}{4} \frac{a_+^2 \langle v_\Pi | v_\Sigma \rangle^2}{\Delta E_{\Pi\Sigma} + A_\Pi} \left\{ \frac{1}{12} \left(\frac{J_0 + 3/2}{J_0} \right) \frac{1}{1 - 4\varepsilon' J_0} + \frac{1}{4} \left(\frac{J_0 - 1/2}{J_0} \right) \right\} \\ &\approx \frac{1}{12} \frac{a_+^2 \langle v_\Pi | v_\Sigma \rangle^2}{\Delta E_{\Pi\Sigma} + A_\Pi} \left[1 + \varepsilon' (J_0 + 3/2) \right], \end{aligned} \tag{61}$$

where $\varepsilon' = B_\Sigma / (\Delta E_{\Pi\Sigma} + A_\Pi)$.

Similarly, for paths 7 and 8, the relevant energy differences are

$$\begin{aligned} E(^4\Sigma^-, J_0, f_1) - E(^4\Sigma^-, J_0, e_1) &= 2B_\Sigma (J_0 - 1/2), \\ E(^4\Sigma^-, J_0 f_2) - E(^4\Sigma^-, J_0, e_1) &= 6B_\Sigma (J_0 + 1/2). \end{aligned} \tag{62}$$

The shift of the f-level is accordingly,

$$\begin{aligned}\delta E_{\Pi(F_1,f)} &= \frac{c_{7a}^2}{\Delta E_{\Pi\Sigma} + A_\Pi - 2B_\Sigma (J_0 - 1/2)} \\ &\quad + \frac{c_{8a}^2}{\Delta E_{\Pi\Sigma} + A_\Pi - 6B_\Sigma (J_0 + 1/2)} \\ &= \frac{1}{4} \frac{a_+^2 \langle v_\Pi | v_\Sigma \rangle^2}{\Delta E_{\Pi\Sigma} + A_\Pi} \left\{ \frac{1}{12} \left(\frac{J_0 - 1/2}{J_0 + 1} \right) \frac{1}{1 - 2\varepsilon' (J_0 - 1/2)} \right. \\ &\quad \left. + \frac{1}{4} \left(\frac{J_0 + 3/2}{J_0 + 1} \right) \frac{1}{1 - 6\varepsilon' (J_0 + 1/2)} \right\} \\ &\approx \frac{1}{12} \frac{a_+^2 \langle v_\Pi | v_\Sigma \rangle^2}{\Delta E_{\Pi\Sigma} + A_\Pi} \left[1 + \varepsilon' (5J_0 + 7/2) \right]. \end{aligned} \tag{63}$$

Combining Eqs. (61) and (63) gives for the Λ-doubling of the F_1 levels:

$$\begin{aligned}\delta E_{\Pi(F_1,f)} - \delta E_{\Pi(F_1,e)} &= \frac{1}{3} \frac{a_+^2 \langle v_\Pi | v_\Sigma \rangle^2}{\Delta E_{\Pi\Sigma} + A_\Pi} \varepsilon' (J_0 + 1/2) \\ &= \frac{2}{3} \frac{a_+^2 \langle v_\Sigma | v_\Pi \rangle^2}{(\Delta E_{\Pi\Sigma} + A_\Pi)^2} B_\Sigma (J_0 + 1/2). \end{aligned} \tag{64}$$

This non-zero splitting of the F_1 levels is in contrast to the zero splitting of the F_2 levels.

F. Calculation of the Λ-doubling: Case (b)

Finally, we turn to the splitting of the $^2\Pi$ levels in the case (b) limit, which are depicted in Fig. 5.

The shift of the e-levels is produced by paths 1, 5, and 6. The result is

$$\delta E_{\Pi(e)} = \frac{c_{1b}^2}{\Delta E_{\Pi\Sigma}} + \frac{c_{5b}^2}{\Delta E_{\Pi\Sigma} + 2B_\Sigma N_0} + \frac{c_{6b}^2}{\Delta E_{\Pi\Sigma} - 2B_\Sigma (N_0 + 1)}, \tag{65}$$

where

$$\Delta E_{\Pi\Sigma}(N_0) = (T_\Pi - T_\Sigma) + (B_\Pi - B_\Sigma) N_0 (N_0 + 1). \tag{66}$$

The shift of the f-levels is produced by paths 3, 4, and 7. The result is

$$\delta E_{\Pi(f)} = \frac{c_{7b}^2}{\Delta E_{\Pi\Sigma}} + \frac{c_{3b}^2}{\Delta E_{\Pi\Sigma} + 2B_\Sigma N_0} + \frac{c_{4b}^2}{\Delta E_{\Pi\Sigma} - 2B_\Sigma (N_0 + 1)}. \tag{67}$$

In the limit of large N_0, the coefficients listed in Table I have the values $c_{1b}^2 = c_{7b}^2 = \frac{1}{6} a_+^2 \langle v_\Pi | v_\Sigma \rangle^2$, $c_{3b}^2 = c_{5b}^2 = \frac{1}{24} a_+^2 \langle v_\Pi | v_\Sigma \rangle^2$, and $c_{4b}^2 = c_{6b}^2 = \frac{1}{8} a_+^2 \langle v_\Pi | v_\Sigma \rangle^2$, and the Λ-doubling, $\delta E_{\Pi(f)} - \delta E_{\Pi(e)}$, vanishes. At intermediate values of N_0, the Λ-doubling is

$$\begin{aligned}\delta E_{\Pi(f)} - \delta E_{\Pi(e)} &\approx \frac{a_+^2 \langle v_\Pi | v_\Sigma \rangle^2}{4\Delta E_{\Pi\Sigma}} \left\{ \frac{2}{3} \frac{N_0 + 1/2}{N_0 (N_0 + 1)} \right. \\ &\quad + \frac{1}{6} \frac{N_0^2 + N_0 + 1}{N_0 (N_0 + 1/2)(N_0 + 1)} (1 - 2\varepsilon) \\ &\quad \left. - \frac{1}{2} \frac{1}{N_0 + 1/2} (1 + 2\varepsilon) \right\} \\ &\approx \frac{a_+^2 \langle v_\Pi | v_\Sigma \rangle^2}{12\, \Delta E_{\Pi\Sigma}\, N_0}. \end{aligned} \tag{68}$$

The Λ-splitting vanishes as $a_+ \to 0$ and $N_0 \to \infty$.

V. SPLITTING OF $^2\Pi$ BY $^2\Sigma^+$

The numerator effect is absent in the examples that we have considered so far because, in those cases, the off-diagonal matrix element of the rotational Hamiltonian is either zero or independent of e/f symmetry. In this section, we show that both the e/f-symmetry dependence of the numerator, which is responsible for the conventional Λ-doubling effect, and the J-dependent denominator effect may exist simultaneously for the same state.

We consider here the perturbation of the $^2\Pi$ state by the $^2\Sigma^+$ state. The conventional Λ-doubling of the OH($X^2\Pi_i$) state has been studied extensively.[15,16] The rotational energy levels of these states are shown schematically in Figs. 6 and 7 for Hund's cases (a) and (b), respectively. There are four possible symmetry-preserving paths, which are named $e_2 - e$, $f_2 - f$, $e_1 - e$, and $f_1 - f$, where the subscripted letter denotes the $^2\Pi$ level, and the unsubscripted letter denotes the $^2\Sigma^+$ level. The matrix elements for these paths [see Eqs. (3.5.28) and (3.5.29) in Ref. 1] are collected in Table II in the Appendix.

Ignoring for the moment the denominator effect, the second-order energy shifts for the $^2\Pi_{\frac{1}{2}}$ state in case (a) are

$$\begin{aligned}\delta E_e &= \left[\frac{1}{4} a_+^2 \langle v_\Pi | v_\Sigma \rangle^2 + B_{v_\Pi, v_\Sigma}^2 b_{\Pi\Sigma}^2 (J - 1/2)^2 \right. \\ &\quad \left. - B_{v_\Pi, v_\Sigma} b_{\Pi\Sigma} a_+ \langle v_\Pi | v_\Sigma \rangle (J - 1/2) \right] / \Delta E, \\ \delta E_f &= \left[\frac{1}{4} a_+^2 \langle v_\Pi | v_\Sigma \rangle^2 + B_{v_\Pi, v_\Sigma}^2 b_{\Pi\Sigma}^2 (J + 3/2)^2 \right. \\ &\quad \left. + B_{v_\Pi, v_\Sigma} b_{\Pi\Sigma} a_+ \langle v_\Pi | v_\Sigma \rangle (J + 3/2) \right] / \Delta E, \end{aligned} \tag{69}$$

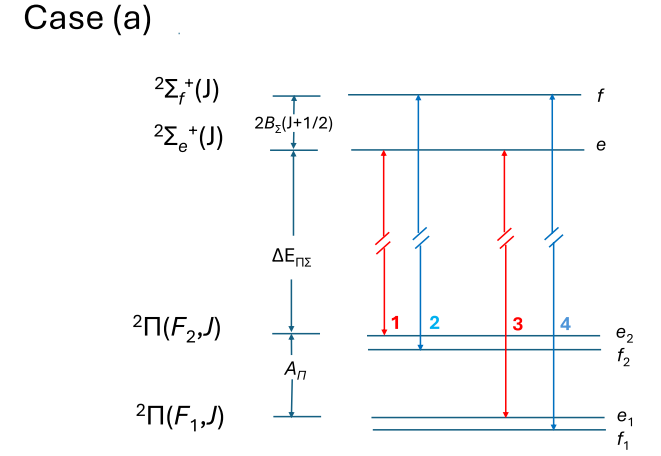

FIG. 6. Diagram of the rotational energy levels of the $^2\Pi$ and $^2\Sigma^+$ states in the case (a) limit of the $^2\Pi$ state. The arrows indicate the symmetry-allowed paths. The path numbers are indicated at the bottom right of each arrow. Paths 1 and 3—shown in red—indicate the interactions of states of *e*-symmetry, and paths 2 and 4—shown in blue—indicate the interactions of states of *f*-symmetry.

where

$$\Delta E = T_\Pi - T_\Sigma + (B_\Pi - B_\Sigma)(J + 1/2), \tag{70}$$

and the second-order Λ-splitting is

$$\delta\nu_\Pi^0 = \left[4B^2_{v_\Pi,v_\Sigma} b^2_{\Pi\Sigma} + 2B_{v_\Pi,v_\Sigma} b_{\Pi\Sigma}\, a_+ \langle v_\Pi|v_\Sigma\rangle\right](J + 1/2)/h\Delta E. \tag{71}$$

For the $^2\Pi_{\frac{3}{2}}$ state (paths 1 and 2), the coefficients c_{1a} and c_{2a} are equal and, accordingly, there is no Λ-splitting.

We derived $\delta\nu_\Pi^0$ by assuming that the $^2\Sigma_e^+$ and $^2\Sigma_f^+$ states are degenerate. But, in fact, their energies, which are obtained by diagonalizing $\hat{\mathscr{H}}^{SU}$ [see Eqs. (3.5.21) and (3.5.22) in Ref. 1], are

$$E(^2\Sigma^+_{e/f}, J) = T_\Sigma + B_\Sigma[J(J + 1) + 1/4 \mp (J + 1/2)], \tag{72}$$

and their difference is

$$E(^2\Sigma_f^+, J) - E(^2\Sigma_e^+, J) = 2B_\Sigma(J + 1/2). \tag{73}$$

This difference stems from the property that the spin-uncoupling matrix element, $\langle {}^2\Sigma^+_{\frac{1}{2}}|\hat{J}^-\hat{S}^+|{}^2\Sigma^+_{-\frac{1}{2}}\rangle = J + 1/2$, is not zero.

A consequence of the energy difference between the $^2\Sigma_f^+$ and $^2\Sigma_e^+$ energies is that the perturbations of the $^2\Pi_f$ and $^2\Pi_e$ states have different energy denominators. This property is accounted for by multiplying δE_f in Eq. (69) by the factor $1 + 2\varepsilon(J + 1/2)$, where $\varepsilon = B_\Sigma/\Delta E$. The total Λ-splitting is given by

$$\delta\nu_\Pi(J) \approx \delta\nu_\Pi^0(J) + \left[\frac{1}{4}a_+^2\langle v_\Pi|v_\Sigma\rangle^2 + B^2_{v_\Pi,v_\Sigma} b^2_{\Pi\Sigma}(J + 3/2)^2 + B_{v_\Pi,v_\Sigma} b_{\Pi\Sigma}\, a_+\langle v_\Pi|v_\Sigma\rangle(J + 3/2)\right]\frac{2\varepsilon(J + 1/2)}{h\Delta E}. \tag{74}$$

In the low-J limit (i.e., $J \ll a_+/4B$), we retain only the first term in the brackets in Eq. (74). The additional splitting caused by the denominator effect is then given by

$$\delta\nu_\Pi(J) - \delta\nu_\Pi^0(J) \approx \frac{1}{2}a_+^2\langle v_\Pi|v_\Sigma\rangle^2 B_\Sigma(J + 1/2)/h(\Delta E)^2. \tag{75}$$

In this limit, $\Delta E \approx T_\Pi - T_\Sigma$, and the ratio of the additional splitting caused by the denominator effect to the total splitting is approximately $-a_+(J + 1/2)/4(T_\Sigma - T_\Pi)$. We note that the contributions to the splitting from both the numerator and denominator are linear in J. These results may be compared to the splitting of $^2\Pi(F_1)$ by $^4\Sigma^+$, which is also linear in J, whereas the splitting of $^1\Pi$ by $^3\Sigma^-$ is quadratic in J, and the splitting of $^1\Delta$ by $^1\Pi$ varies as the fourth power of J.

In the case (b) limit, we define a pattern forming quantum number, N, such that $N = J - 1/2$ for states of *e*-symmetry and $N = J + 1/2$ for states of *f*-symmetry. Equation (72) shows that the rotational energy levels of the $^2\Sigma^+$ state are two-fold degenerate, with energies $E(^2\Sigma^+, N, e) = E(^2\Sigma^+, N, f) = B_\Sigma N(N + 1)$. These energy

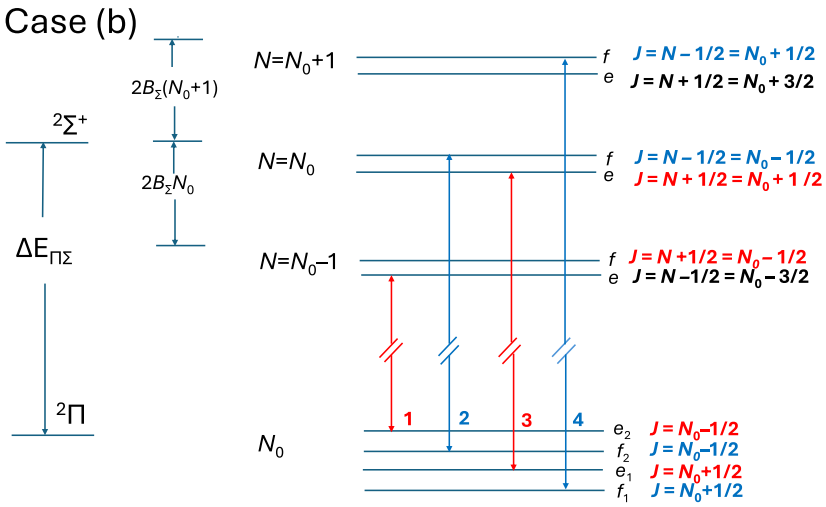

FIG. 7. Diagram of the rotational energy levels of the $^2\Pi$ and $^2\Sigma^+$ states in the case (b) limit of the $^2\Pi$ state. The arrows indicate the symmetry-allowed paths. The path numbers are indicated at the bottom right of each arrow. Paths 1 and 3—shown in red—indicate the interactions of states of *e*-symmetry, and paths 2 and 4—shown in blue—indicate the interactions of states of *f*-symmetry.

TABLE II. Matrix elements for the perturbation paths connecting the $^2\Pi$ and $^2\Sigma^+$ states.

Path	$\langle {}^2\Pi(a)\vert \hat{\mathscr{H}}^{Rot} + \hat{\mathscr{H}}^{SO} \vert {}^2\Sigma^+\rangle$	$\langle {}^2\Pi(b)\vert \hat{\mathscr{H}}^{Rot} + \hat{\mathscr{H}}^{SO} \vert {}^2\Sigma^+\rangle$
(1) $e_2 - e$	$-b_{\Sigma,\Pi}\, B_{v_\Sigma,v_\Pi}\sqrt{(J-1/2)(J+3/2)}$	$\left(\frac{N_0+1}{N_0}\right)^{\frac{1}{2}} 2^{-\frac{3}{2}}\, a_+\langle v_\Pi\vert v_\Sigma\rangle$
(2) $f_2 - f$	$-b_{\Sigma,\Pi}\, B_{v_\Sigma,v_\Pi}\sqrt{(J-1/2)(J+3/2)}$	$\left(\frac{N_0+1}{N_0}\right)^{\frac{1}{2}}\left[2^{\frac{1}{2}}\, b_{\Sigma,\Pi}\, B_{v_\Sigma,v_\Pi} N_0 + 2^{-\frac{3}{2}}\, a_+\langle v_\Pi\vert v_\Sigma\rangle\right]$
(3) $e_1 - e$	$-b_{\Sigma,\Pi}\, B_{v_\Sigma,v_\Pi}(J-1/2) + a_+\langle v_\Pi\vert v_\Sigma\rangle/2$	$\left(\frac{N_0}{N_0+1}\right)^{\frac{1}{2}}\left[-2^{\frac{1}{2}}\, b_{\Sigma,\Pi}\, B_{v_\Sigma,v_\Pi}(N_0+1) + 2^{-\frac{3}{2}}\, a_+\langle v_\Pi\vert v_\Sigma\rangle\right]$
(4) $f_1 - f$	$b_{\Sigma,\Pi}\, B_{v_\Sigma,v_\Pi}(J+3/2) + a_+\langle v_\Pi\vert v_\Sigma\rangle/2$	$\left(\frac{N_0}{N_0+1}\right)^{\frac{1}{2}} 2^{-\frac{3}{2}}\, a_+\langle v_\Pi\vert v_\Sigma\rangle$

levels are shown schematically in Fig. 7 for three consecutive values of N.

The energy shifts produced by the four paths are

$$\delta E_e = \frac{c_{1b}^2}{\Delta E_{\Pi\Sigma} + 2B_\Sigma N_0} + \frac{c_{3b}^2}{\Delta E_{\Pi\Sigma}} \approx \frac{c_{1b}^2(1-2\varepsilon N_0)}{\Delta E_{\Pi\Sigma}} + \frac{c_{3b}^2}{\Delta E_{\Pi\Sigma}},$$
$$\delta E_f = \frac{c_{4b}^2}{\Delta E_{\Pi\Sigma} - 2B_\Sigma(N_0+1)} + \frac{c_{2b}^2}{\Delta E_{\Pi\Sigma}} \approx \frac{c_{4b}^2[1+2\varepsilon(N_0+1)]}{\Delta E_{\Pi\Sigma}} + \frac{c_{2b}^2}{\Delta E_{\Pi\Sigma}}. \quad (76)$$

It is apparent that the denominator effect in case (b) is produced by paths 1 and 4. After some algebra, we obtain for the Λ-doubling

$$\delta\nu_\Pi = \delta\nu_f - \delta\nu_e = \left\{-\frac{1}{N_0} + 2\varepsilon(N_0+1/2)\right\}\xi^2/h\Delta E_{\Pi\Sigma} + \left\{-\frac{1}{N_0}\xi^2 \pm 4B_{v_\Pi,v_\Sigma} b_{\Pi\Sigma}\, \xi(N_0+1/2)\right\}/h\Delta E_{\Pi\Sigma}, \quad (77)$$

where the ± signs correspond to regular ($A_\Pi > 0$) and inverted ($A_\Pi < 0$) $^2\Pi$ states, respectively. (Here and in the following equation, we use the notation $\xi \equiv a_+\langle v_\Pi\vert v_\Sigma\rangle/2$.) The first term on the right-hand side of Eq. (77) is the contribution from the denominator, and the second term is the contribution from the numerator. The ratio of the contributions from the denominator and numerator is

$$\frac{\left[-\frac{1}{N_0} + 2\varepsilon(N_0+1/2)\right]\xi}{-\frac{\xi}{N_0} \pm 4B_{v_\Pi,v_\Sigma} b_{\Pi\Sigma}(N_0+1/2)} \approx \pm\frac{\varepsilon\,\xi}{2B_{v_\Pi,v_\Sigma} b_{\Pi\Sigma}} = \pm\frac{a_+}{4b_{\Pi\Sigma}\,\Delta E_{\Pi\Sigma}}. \quad (78)$$

We find that the denominator effect depends very weakly on N and vanishes in the case (b) limit when $a_+ \to 0$.

VI. SUMMARY AND CONCLUSIONS

The second-order energy shift of a rotational level that is perturbed by an energetically remote electronic state is given by the square of the matrix element of the perturbing terms in the Hamiltonian divided by the energy difference between the perturbed and perturbing states. With the exception of $^2\Sigma$ states, unperturbed rotational states that differ only in their e/f-symmetry are degenerate. The lifting of this degeneracy by an electronic perturbation is known as Λ-doubling. The conventional explanation of Λ-doubling is that it is caused by the e/f-symmetry dependence of the off-diagonal matrix element in the numerator of the perturbation expression.

In this study, we have shown that Λ-doubling may also have contributions from the energy denominator. The symmetry dependence of the denominator is a consequence of the requirements that the perturbed and perturbing states have both the same e/f-symmetry and the same total angular momentum, J. Satisfaction of these two requirements leads to the possibility that either the rotational or the electronic energy of the perturbing state may be e/f symmetry-dependent. The denominator effect is important because it can lift the degeneracy of a state even when the matrix elements of the perturbing terms in the Hamiltonian are independent of e/f symmetry.

In this study, we provide six examples of how the e/f-symmetry of the denominator can arise, as follows:

(i) In the perturbation of $^1\Pi$ by $^3\Sigma^-$ states, there are three paths: two with e-symmetry and one with f-symmetry. The larger number of paths with e-symmetry produces a net splitting. Figure 1 shows that the energy difference of these paths follows from the e/f-symmetry of the rotational levels of the $^3\Sigma^-$ states. An example where denominator effects may be important is the perturbation of the $A^1\Pi$ state of CO.[17] In that case, the full effective Hamiltonian includes all of the perturbing states, and the denominator effects from very remote perturbing states cannot be distinguished from numerator effects.

(ii) In the perturbation of $^1\Delta_2$ by $^1\Pi$ states, there are two energy paths: one with e-symmetry and one with f-symmetry. The energy difference of these paths is a consequence of the Λ-doubling of the $^1\Pi$ state. Lambda-doubling of the $^1\Delta$ state is, therefore, a higher order consequence of the symmetry dependence of the rotational levels of the $^1\Pi$ states. We note that, as shown in Ref. 11, the $^1\Delta_2$ state can also be split directly by a Σ state.

(iii) In the perturbation of the F_1 levels of the $^2\Pi$ state by the $^2\Sigma^+$ state, there are again only two energy paths: one with e-symmetry and one with f-symmetry. Figure 6 shows that the energy difference of these paths is a consequence of the electronic energy difference between the $^2\Sigma_f^+$ and $^2\Sigma_e^+$ states. This energy difference is produced by the spin-uncoupling terms in the Hamiltonian. The same effect occurs for the F_2

levels of a $^2\Pi$ state. For these perturbations, both numerator and denominator effects exist simultaneously.

(iv) In the case (b) splitting of the $^2\Pi$ state by the $^2\Sigma^+$ state, there are four paths, two of each symmetry. The splitting depends very weakly on N and vanishes when a_+ goes to zero.

(v) In the perturbation of the F_1 levels of the $^2\Pi$ state by the $^4\Sigma^-$ state, there are four energy paths: two with e-symmetry and two with f-symmetry. Figure 3 shows that the energy differences of these paths are a consequence of the rotational properties of the $^4\Sigma^-$ state. The same is true for the F_2 levels of $^2\Pi$ state.

(vi) Finally, in the case (b) splitting of the $^2\Pi$ state by the $^4\Sigma^-$ state, there are six paths, three of each symmetry. This splitting depends very weakly on N and vanishes when either $a_+ = 0$ or $N \to \infty$.

The main finding of this study is that Λ-doubling may be significant even where there is no rotational interaction (e.g., for $\Delta S \neq 0$), or when the off-diagonal matrix element of $\hat{\mathscr{H}}^{Rot}$ is independent of e/f-symmetry. We have shown that the Λ-doubling for $^1\Pi \sim {}^3\Sigma^-$ is proportional to $a_+^2B^2J^2/(\Delta E)^2$ [see Eq. (26)]; for $^1\Delta \sim {}^1\Pi$, it is proportional to $a_+^2B^4J^4/(\Delta E)^4$ [see Eq. (33)]; and for $^2\Pi(F_1) \sim {}^4\Sigma^-$, it is proportional to $a_+^2BJ/(\Delta E + A)^2$ [see Eq. (64)].

When the spin–orbit interaction is strong, the energy denominator effects are large and systematically observable. This is especially true for molecules containing heavy atoms, where Hund's case (c) is applicable. In that case, the spin quantum number is not specified, and Λ-doubling is replaced by Ω-doubling. For this type of doubling, which has not been systematically studied, e/f-splitting will provide a spectrum-only path toward reconstruction of partial L, Λ, and S characters of the states. The denominator effect may also play a major role in the Λ-doubling of high Rydberg states, where the energy spacing between electronic states is small.

ACKNOWLEDGMENTS

No external funding was used for this study.

AUTHOR DECLARATIONS

Conflict of Interest

The authors have no conflicts to disclose.

Author Contributions

Robert J. Gordon: Conceptualization (equal); Formal analysis (equal); Investigation (equal); Methodology (equal); Project administration (equal); Software (equal); Writing – original draft (equal); Writing – review & editing (equal). **Robert W. Field**: Conceptualization (equal); Formal analysis (equal); Investigation (equal); Methodology (equal); Project administration (equal); Software (equal); Writing – original draft (equal); Writing – review & editing (equal).

DATA AVAILABILITY

All required data are included within the text.

APPENDIX: OFF-DIAGONAL MATRIX ELEMENTS OF $\hat{\mathscr{H}}^{SO} + \hat{\mathscr{H}}^{Rot}$

For three electrons, the electronic configuration of a regular $^2\Pi$ state is $\sigma^2\pi$, and for an inverted $^2\Pi$ state, it is π^3. The electronic wave functions for these states are given by the following combinations of Slater determinants:

$$
\begin{aligned}
|^2\Pi_{\frac{1}{2}}, J, \sigma^2\pi\rangle_{e,f} &= \frac{1}{\sqrt{2}}\left[|\pi^+\beta, \sigma\alpha, \sigma\beta||J, 1/2\rangle \pm |\pi^-\alpha, \sigma\alpha, \sigma\beta||J, -1/2\rangle\right],\\
|^2\Pi_{\frac{3}{2}}, J, \sigma^2\pi\rangle_{e,f} &= \frac{1}{\sqrt{2}}\left[|\pi^+\alpha, \sigma\alpha, \sigma\beta||J, 1/2\rangle \pm |\pi^-\alpha, \sigma\alpha, \sigma\beta||J, -1/2\rangle\right],\\
|^2\Pi_{\frac{1}{2}}, J, \pi^3\rangle_{e,f} &= \frac{1}{\sqrt{2}}\big[|\pi^+\alpha, \pi^+\beta, \pi^-\beta||J, 1/2\rangle\\
&\quad \pm |\pi^+\alpha, \pi^-\alpha, \pi^-\beta||J, -1/2\rangle\big],\\
|^2\Pi_{\frac{3}{2}}, J, \pi^3\rangle_{e,f} &= \frac{1}{\sqrt{2}}\big[|\pi^+\alpha, \pi^+\beta, \pi^-\alpha||J, 1/2\rangle\\
&\quad \pm |\pi^+\beta, \pi^-\alpha, \pi^-\beta||J, -1/2\rangle\big].
\end{aligned}
\tag{A1}
$$

The wave functions for the components of $^2\Sigma^\pm$ and $^4\Sigma^\pm$ states are

$$
\begin{aligned}
|^2\Sigma^+_{\frac{1}{2}}, J\rangle_{e,f} &= \frac{1}{2}\left[(|\pi^+\alpha, \pi^-\beta, \sigma\alpha| - |\pi^+\beta, \pi^-\alpha, \sigma\alpha|)|J, 1/2\rangle\right] \pm (|\pi^+\alpha, \pi^-\beta, \sigma\beta| - |\pi^+\beta, \pi^-\alpha, \sigma\beta|)|J, -1/2\rangle\Big],\\
|^2\Sigma^-_{\frac{1}{2}}, J\rangle_{e,f} &= \frac{1}{\sqrt{12}}\big[(2|\pi^+\alpha, \pi^-\alpha, \sigma\beta| - |\pi^+\alpha, \pi^-\beta, \sigma\alpha| - |\pi^+\beta, \pi^-\alpha, \sigma\alpha|)|J, 1/2\rangle\\
&\quad \pm (2|\pi^+\beta, \pi^-\beta, \sigma\alpha| - |\pi^+\alpha, \pi^-\beta, \sigma\beta| - |\pi^+\beta, \pi^-\alpha, \sigma\beta|)|J, -1/2\rangle\big],\\
|^4\Sigma^-_{\frac{1}{2}}, J\rangle_{e,f} &= \frac{1}{\sqrt{6}}\big[(|\pi^+\alpha, \pi^-\alpha, \sigma\beta| + |\pi^+\alpha, \pi^-\beta, \sigma\alpha| + |\pi^+\beta, \pi^-\alpha, \sigma\alpha|)|J, 1/2\rangle\\
&\quad \pm (|\pi^+\beta, \pi^-\beta, \sigma\alpha| + |\pi^+\alpha, \pi^-\beta, \sigma\beta| + |\pi^+\beta, \pi^-\alpha, \sigma\beta|)|J, -1/2\rangle\big],\\
|^4\Sigma^-_{\frac{3}{2}}, J\rangle_{e,f} &= \frac{1}{\sqrt{2}}\left[|\pi^+\alpha, \pi^-\alpha, \sigma\alpha||J, 3/2\rangle \pm |\pi^+\beta, \pi^-\beta, \sigma\beta||J, -3/2\rangle\right].
\end{aligned}
\tag{A2}
$$

Using these wave functions, we calculate the matrix elements of the spin–orbit operator for both the $\sigma^2\pi$ and π^3 configurations. The results are

$$\begin{aligned}
\langle {}^2\Pi_{\frac{3}{2}}, \sigma^2\pi|\hat{\mathscr{H}}^{SO}|{}^4\Sigma^-_{\frac{3}{2}}\rangle &= \frac{1}{2}\langle|\pi^+\alpha,\sigma\alpha,\sigma\beta||\hat{a}\hat{\ell}^+_2\hat{s}_2{}^-||\pi^+\alpha,\pi^-\alpha,\sigma\alpha|\rangle = -a_+\langle \mathrm{v}|\Pi\mathrm{v}_\Sigma\rangle/2,\\
\langle {}^2\Pi_{\frac{3}{2}}, \pi^3|\hat{\mathscr{H}}^{SO}|{}^4\Sigma^-_{\frac{3}{2}}\rangle &= \frac{1}{2}\langle|\pi^+\alpha,\pi^+\beta,\pi^-\alpha||\hat{a}\hat{\ell}^+_3\hat{s}_3{}^-||\pi^+\alpha,\pi^-\alpha,\sigma\alpha|\rangle = -a_+\langle \mathrm{v}|\Pi\mathrm{v}_\Sigma\rangle/2,\\
\langle {}^2\Pi_{\frac{1}{2}}, \sigma^2\pi|\hat{\mathscr{H}}^{SO}|{}^4\Sigma^-_{\frac{1}{2}}\rangle &= \frac{1}{2}\frac{1}{\sqrt{3}}\langle|\pi^+\beta,\sigma\alpha,\sigma\beta||\hat{a}\hat{\ell}^+_2\hat{s}_2{}^-\times\left[||\pi^+\alpha,\pi^-\alpha,\sigma\beta| + |\pi^+\alpha,\pi^-\beta,\sigma\alpha| + \underline{|\pi^+\beta,\pi^-\alpha,\sigma\alpha|}\rangle\right] = \frac{1}{2\sqrt{3}}\,a_+\langle \mathrm{v}|\Pi\mathrm{v}_\Sigma\rangle,\\
\langle {}^2\Pi_{\frac{1}{2}}, \pi^3|\hat{\mathscr{H}}^{SO}|{}^4\Sigma^-_{\frac{1}{2}}\rangle &= \frac{1}{2}\frac{1}{\sqrt{3}}\langle|\pi^+\alpha,\pi^+\beta,\pi^-\alpha||\hat{a}\hat{\ell}^+_3\hat{s}_3{}^-\times\left[\underline{||\pi^+\alpha,\pi^-\alpha,\sigma\beta|} + |\pi^+\alpha,\pi^-\beta,\sigma\alpha| + |\pi^+\beta,\pi^-\alpha,\sigma\alpha|\rangle\right]\\
&= -\frac{1}{2\sqrt{3}}\,a_+\langle \mathrm{v}|\Pi\mathrm{v}_\Sigma\rangle.
\end{aligned} \tag{A3}$$

The factor of $\sqrt{3}$ is a consequence of the presence of three Slater determinants for the ${}^4\Sigma^-_{\frac{1}{2}}$ state, only one of which [underlined in Eq. (A3)] has a non-zero matrix element. The minus signs on the right-hand sides of these equations come from rearranging the spin-orbitals into standard order after operation by $\hat{\mathscr{H}}^{SO}$.

Next, we derive the off-diagonal matrix elements that appear in the numerator of the perturbation expression. We consider first the perturbation of the ${}^2\Pi$ state by the ${}^4\Sigma^-$ state. For this case, where $\Delta S \neq 0$, the matrix elements of $\hat{\mathscr{H}}^{Rot}$ are zero. From Eq. (A3), we know that $\langle {}^2\Pi_{\frac{1}{2}}|\hat{\mathscr{H}}^{SO}|{}^4\Sigma^-_{\frac{3}{2}}\rangle = -a_+\langle \mathrm{v}_\Pi|\mathrm{v}_\Sigma\rangle/2\sqrt{3}$ and $\langle {}^2\Pi_{\frac{1}{2}}|\hat{\mathscr{H}}^{SO}|{}^4\Sigma^-_{\frac{3}{2}}\rangle = -a_+\langle \mathrm{v}_\Pi|\mathrm{v}_\Sigma\rangle/2$. We then use the electronic/rotational wave functions for $|{}^2\Pi, J\rangle_{e,f}$ given by Eq. (51) and the wave functions for $|{}^4\Sigma^-_{e,f}\rangle_{e,f}$ given by Eqs. (35) and (37) to calculate the off-diagonal matrix elements of $\hat{\mathscr{H}}^{SO}$. The results are given in Table I.

The paths listed in column 1 of this table correspond to the numbered arrows in Fig. 3. The matrix elements in columns 2 and 3 correspond to Hund's cases (a) and (b) for the ${}^2\Pi$ state, respectively. They are consistent with Eqs. (4.3.2-5) and (4.3.2-6) in Ref. 9. In column 4, the matrix elements for case (b) are expressed as functions of the pattern-forming quantum number, N_0. The relation between N for the ${}^4\Sigma^-$ state and N_0 for the ${}^2\Pi$ state is obtained from Eqs. (38) and (52). These equations yield $N = N_0 - 1$ for F_{1e}, $N = N_0$ for F_{1f} and F_{2e}, and $N = N_0 + 1$ for F_{2f}.

The matrix elements in column 2 of Table I are labeled c_{1a} ... c_{8a} in the body of the paper, and those in columns 3 and 4 are labeled c_{1b} ... c_{8b} in the body of the paper. We illustrate the calculation of the matrix elements for path 6. For case (a), the ${}^2\Pi(e_1)$ wave function is $|{}^2\Pi_{1/2}\rangle$, and the matrix element equals $-a_+\langle \mathrm{v}_\Pi|\mathrm{v}_\Sigma\rangle/2\sqrt{3}$ times the coefficient of the ${}^4\Sigma^-_{\frac{1}{2}}$ function. For the $e_1 - e_1$ path, the result is

$$c_{6a} = -\frac{a_+\langle \mathrm{v}_\Pi|\mathrm{v}_\Sigma\rangle/2}{\sqrt{3}}\sqrt{\frac{3(J-1/2)}{4J}} = -\frac{1}{4}\sqrt{\frac{J-1/2}{4J}}\,a_+\langle \mathrm{v}_\Pi|\mathrm{v}_\Sigma\rangle. \tag{A4}$$

Replacing J by $N_0 + 1/2$ gives the value of c_{6a} in the table.

For case (b), the ${}^2\Pi$ wave function is given by Eq. (51), and the matrix element listed in Table I is

$$\begin{aligned}
c_{6b} &= -\frac{a_+\langle \mathrm{v}_\Pi|\mathrm{v}_\Sigma\rangle/2}{\sqrt{3}}\sqrt{\frac{3(J-1/2)}{2(J+1/2)}}\sqrt{\frac{J-1/2}{4J}}\\
&\quad - a_+\langle \mathrm{v}_\Pi|\mathrm{v}_\Sigma\rangle/2\sqrt{\frac{J+3/2}{2(J+1/2)}}\sqrt{\frac{J+3/2}{4J}}\\
&= -\sqrt{\frac{1}{2}}\sqrt{\frac{J+1/2}{J}}\,a_+\langle \mathrm{v}_\Pi|\mathrm{v}_\Sigma\rangle/2.
\end{aligned} \tag{A5}$$

Setting $J = N_0 + 1/2$ gives the value of c_{6b} listed in the table.

We confirm by explicit calculation of these matrix elements that $\langle {}^2\Pi(b)|\hat{\mathscr{H}}^{SO}|{}^4\Sigma^-\rangle = 0$ for paths 2 and 8 (which are intentionally missing in Fig. 5), in accord with the selection rule $\Delta N = 0, \pm 1$ for case (b).

The matrix elements for the perturbation of ${}^2\Pi$ state by the ${}^2\Sigma^+$ state are calculated in a similar fashion and are listed in Table II. The matrix elements in this table are for the regular ${}^2\Pi$ state. For the inverted state, a_+ should be replaced by $-a_+$, and c_{3a} and c_{4a} should be interchanged.

REFERENCES

[1] H. Lefebvre-Brion and R. W. Field, *The Spectra and Dynamics of Diatomic Molecules* (Elsevier, Amsterdam, 2004).
[2] J. M. Brown and A. Carington, *Rotational Spectroscopy of Diatomic Molecules* (Cambridge, Cambridge, 2003).
[3] R. N. Zare, *Angular Momentum: Understanding Spatial Aspects in Chemistry and Physics* (Wiley, 1988).
[4] J. T. Hougen, *The Calculation of Rotational Energy Levels and Rotational Line Intensities in Diatomic Molecules*, *National Bureau of Standards Monograph* (U.S. Gov. Printing Office, Washington, 1970), Vol. 115.
[5] J. M. Brown, J. T. Hougen, K.-P. Huber, J. W. C. Johns, I. Kopp, H. Lefebvre-Brion, A. J. Merer, D. A. Ramsay, J. Rostas, and R. N. Zare, J. Mol. Spectrosc. **55**, 500 (1975).
[6] J. H. Van Vleck, Phys. Rev. **33**, 467 (1929).
[7] R. S. Mulliken and A. Christy, Phys. Rev. **38**, 87 (1931).
[8] See p. 191 of Ref. 1.
[9] I. Kovacs, *Rotational Structure in the Spectra of Diatomic Molecules* (American Elsevier, New York, 1970).
[10] This result is equivalent to the matrix elements in Sec. 4.3.1 of Ref. 9, apart from an inconsequential reversal of signs for F_{1f} and F_{2e} and the notation used there of $\xi = a_+\langle \mathrm{v}_\Pi|\mathrm{v}_\Sigma\rangle/2$.
[11] J. M. Brown, A. S.-C. Cheung, and A. J. Merer, J. Mol. Spectrosc. **124**, 464 (1987).

[12] Figure 2 is a relabeled version of Fig. 4.68 in Ref. 9, where the correspondence between c/d and e/f symmetries is incorrect.
[13] See Ref. 5 for a discussion of the replacement of c, d by e, f notation and p. 132 of Ref. 1 for a discussion of the F_i notation.
[14] E. Hill and J. H. Van Vleck, Phys. Rev. **32**, 250 (1928).
[15] J. A. Coxon, K. V. L. N. Sastry, J. A. Austin, and D. H. Levy, Can. J. Phys. **57**, 619 (1979).
[16] J. A. Coxon, Can. J. Phys. **58**, 933 (1980).
[17] R. W. Field, B. G. Wicke, J. D. Simmons, and S. G. Tilford, J. Mol. Spectrosc. **44**, 383 (1972).